8
Photopolymers for Multiphoton Lithography in Biomaterials and Hydrogels

Mark W. Tibbitt, Jared A. Shadish, and Cole A. DeForest

8.1
Introduction

The advent of the polymer industry in the 1950s introduced a vast array of novel materials that have impacted all areas of life [1]. Today, polymers and polymerization reactions are utilized additionally in a range of biomedical applications, including as drug delivery systems [2], tissue engineering scaffolds [3], and as medical devices [4]. These biomedical applications have flourished as the available polymer chemistries and processing techniques have matured, enabling the creation of materials that can be tailored specifically for each use. In particular, advances in synthetic chemistry and photophysics have provided the tools needed to initiate and propagate polymerization reactions with light in a controlled manner [5, 6]. The use of light as the catalyst for polymerization provides the experimenter with an unprecedented level of spatial and temporal control over the reaction. That is, the reaction proceeds only where and when the user desires, allowing for facile production of geometrically defined polymeric materials on demand. Additionally, photopolymerization, which we define generally as the class of reactions that transforms solutions of low molecular weight monomers or prepolymers into high molecular weight species or crosslinked networks upon exposure to visible, ultraviolet (UV), or infrared (IR) light, affords high reaction rates under ambient conditions with relatively low energy input in both non-aqueous and aqueous solutions. To clarify, in this chapter photopolymerization will be used predominantly to describe the photocrosslinking of liquid precursors into solid or viscoelastic materials. Photopolymerization reactions have been leveraged within the biomaterials community to address niche design constraints, such as defined geometries (e.g., bone implants) or post-application sol–gel transition (e.g., *in situ* curing hydrogels) [7]. Concurrently, multiphoton lithography (MPL) techniques have been applied in photopolymerization, and the necessary tools are becoming more widely available to the biomedical community. In this chapter, we discuss, review, and provide perspective on the intersection between MPL and photopolymerization for biomaterials with a special emphasis

Multiphoton Lithography: Techniques, Materials and Applications, First Edition.
Edited by Jürgen Stampfl, Robert Liska, and Aleksandr Ovsianikov.

on the chemistries, platforms, and techniques that are relevant to the biological context.

Photopolymerizations have been instrumental in the advancement of several modern industries, including coatings and adhesives, integrated circuits, and optics, on account of their unique properties [8, 9]. Historically, the ancient Egyptians were the first to explore photopolymerization reactions as they utilized sunlight to crosslink oil-soaked linens to create environmental barriers during mummification [10]. In recent decades, photopolymerizations have been leveraged within modern medicine to fabricate biocompatible networks and hydrogels from monomers and end-functional polymers [11]. Here, networks refer to crosslinked polymeric materials that are utilized in the non-solvated state, whereas hydrogels refer to water-swollen crosslinked polymeric materials. The high swelling degree of hydrogels makes them attractive for biomedical applications, as they mimic the mechanical properties of tissues within the body and afford facile transport or nutrients, waste, and signaling molecules [12]. In either case, the spatial and temporal control afforded by photopolymerization enables the production of highly structured materials with predefined geometries and the ability to polymerize *in situ*. Photopolymerized biomaterials have been successfully implemented as barriers, cell delivery vehicles, tissue engineering scaffolds, and drug delivery systems [11].

For many applications, it is desirable to achieve increased feature resolution within 3D objects. Highly ordered or structured materials play an essential role in many modern technologies, including microprocessors, photonics, and optics [13]. Demands in these industries push for increased information content or feature density, which has fostered innovation in the materials science community to write micro- and nanoscale features into functional materials with high fidelity [14]. Photolithography and stereolithography remain the most accessible techniques for rapid and reliable fabrication at the micrometer scale for the fabrication of functional biomaterials. However, as our knowledge of biological systems is increasing, it is becoming clear that traditional monolithic photopolymerization reactions fail to provide materials with the information content needed for all applications. For example, the extracellular matrix (ECM), that is, the local environment that supports and instructs cell function, possesses a high degree of complexity with nanometer- and micrometer-scale architecture that varies with time [15]. Therefore, technologies used for *ex vivo* organ growth, three-dimensional (3D) cell culture, or as injectable cell carriers could all benefit by adopting strategies developed for high-content feature patterning in other industries.

Traditional photopolymerizations employed for biomaterial fabrication are often accessed through a photo-induced free-radical polymerization [16]. This approach minimally requires a precursor solution containing multifunctional monomers and a photoinitiator, as well as an appropriate light source (a comprehensive overview of these components is provided in Section 8.4). Photopolymerized materials are then fabricated by irradiating the precursor solution with light. Molds or masks constrain the geometry, while the dosage and intensity of the light control the extent and kinetics of reaction, respectively [17]. *In vivo*

photopolymerization (or *in situ* photopolymerization) is achieved similarly by placing the precursor solution into the appropriate location within the body, and subsequently initiating the polymerization with light [18]. In this manner, biomaterials can be fabricated rapidly that conform to desired tissue geometries. Alternatively, interfacial photopolymerizations are achieved by adsorbing or grafting a photoinitiator to a biomaterial surface from which a photopolymerized surface or brush can be generated [19]. These approaches enable conformal coatings, molded materials, or *in vivo* implants; however, none of these approaches exploits the full 3D and spatiotemporal resolution that photoinitiation affords, as they are confined to planar patterning.

Increased spatial resolution has been achieved by leveraging photolithography techniques used extensively in the microelectronics industry for the fabrication of integrated circuits [20]. Here, a photomask is used to selectively constrain illumination of the underlying precursor solution. Regions of illumination are photopolymerized into insoluble blocks, while the other nonpolymerized regions can be washed away post fabrication. In this manner, the user can generate defined planar geometries with micrometer-scale resolution and access 3D structures with layer-by-layer fabrication [21]. However, photolithography requires high-resolution photomasks for each geometry, remains diffraction-limited, and can form only simple 3D structures. Soft lithography can also be adapted to photopolymerizations [22]. Here, a master mold is formed in an elastomeric material, such as polydimethylsiloxane (PDMS), with a desired geometry. The mold is filled with a precursor solution, which is photopolymerized to recover the desired features. This approach has been applied to microfabricate biomaterials for drug delivery [23], tissue engineering [24], and microfluidic biosensing [25]. Soft lithography is also limited in that it requires a master mold tailored for each application and involves a multistep process to achieve micrometer-scale materials. An alternative approach for rapid prototyping and micrometer-scale material fabrication is laser scanning lithography (LSL)-based photopolymerization, whereby the focal point of a laser is rastered or serially scanned through defined regions of a precursor solution [26]. Photoinitiation occurs only where the solution is illuminated by the focused laser light, which provides the necessary photons to drive polymerization. On account of scattering and attenuation of the focused laser light, LSL is typically confined to the surface of the precursor solution. In this manner, 3D objects can be generated adopting stereolithographic techniques, whereby an automated stage with *xyz* control moves the object through the focal point of the laser. Layer-by-layer photolithography and LSL combined with stereolithography are currently utilized in the 3D printing industry. In each of these approaches, material fabrication remains limited in spatial resolution to the micrometer scale and fails to access easily all arbitrary 3D geometries.

Specifically, developments in multiphoton technologies have made ultrafast lasers increasingly accessible to the materials science, biology, and biomaterials communities. As a result, researchers have begun to explore the use of multiphoton irradiation to facilitate nanometer- and micrometer-scale phenomena

within the photopolymerization and biological context [27]. MPL – the use of ultrafast, multiphoton lasers to execute LSL – enables the experimenter to photopolymerize materials with feature content down to the nanoscale in three dimensions with high fidelity, owing to the narrow focal region of a multiphoton laser and minimal radical generation outside of the focal spot [28]. In this chapter, we will discuss, review, and provide perspective on the use of MPL as a technique for the fabrication and modification of biomaterials and hydrogels with special emphasis on the photopolymers and techniques that can be performed in or are amenable to the biological context.

8.2 Multiphoton Lithography (MPL) for Photopolymerization

The theory of multiphoton excitation was described initially by Maria Goeppert-Mayer in her doctorate dissertation; Goeppert-Mayer is also the recipient of the 1963 Nobel Prize for Physics for articulating the nuclear shell model of atomic nuclei [29]. The principle of multiphoton excitation, as proposed by Goeppert-Mayer, allows a photoactive molecule to enter an excited state by absorbing multiple photons of lesser energy (longer wavelength) than a single photon of greater energy (shorter wavelength) that would normally result in photoexcitation [29]. This phenomenon, now well tested and established, is traditionally achieved with two photons from the same laser possessing roughly half the energy of a single photon capable of excitation [29]. As both photons are needed to bump the molecule into the excited quantum state, they must both be absorbed within femtoseconds of each other. This is achieved most commonly with high-energy femtosecond pulsed laser sources that significantly increase the probability of absorbing multiple photons nearly simultaneously within the focal volume [30]. Owing to the nonlinear nature of the two photon process, the probability of excitation decays as a function of distance from the focal plane with quadratic dependence, which compresses the axial spread of the point spread function [30]. In practical terms, this means that nearly all of the excitation is confined to the focal plane, providing high resolution (<1 μm) in the axial or *z*-dimension (Figure 8.1a). Assuming reasonable optics, this translates to sub-femtoliter focal volumes. For additional reading, the concepts and physics behind multiphoton excitation are handled with sufficient rigor in Part I and Chapter 6.

Multiphoton techniques were first introduced into the biology and biomaterials communities through the development and proliferation of multiphoton microscopy (MPM) by Watt and colleagues [34, 35]. MPM is now widely available and an attractive tool for high-resolution fluorescent imaging in thick tissues as well as in live animals [30]. Beyond fluorescent imaging, multiphoton excitation is commonly employed for molecular uncaging of small molecules [36], fluorescence recovery after photobleaching (FRAP) [37], and biophysical investigations [38]. Importantly, multiphoton excitation has been incorporated directly into

traditional laser scanning microscopes (LSMs) or LSL setups to image or fabricate materials with micrometer- and nanometer-scale features.

As multiphoton systems have become increasingly accessible, they have been adopted by the materials science and polymers community for high-resolution 3D photopolymerizations [28]. MPL has successfully generated a range of complex, 3D photopolymerized structures (Figure 8.1). The same principles above apply to photopolymerization reactions: if two photons with lesser energy are absorbed by the same photoinitiator nearly simultaneously, the molecule may undergo cleavage and generate initiating radicals within the sub-femtoliter focal volume [28]. Accordingly, rapid prototyping with MPL affords the fabrication of objects with sub-micrometer feature sizes. Initial work has explored the fabrication of open

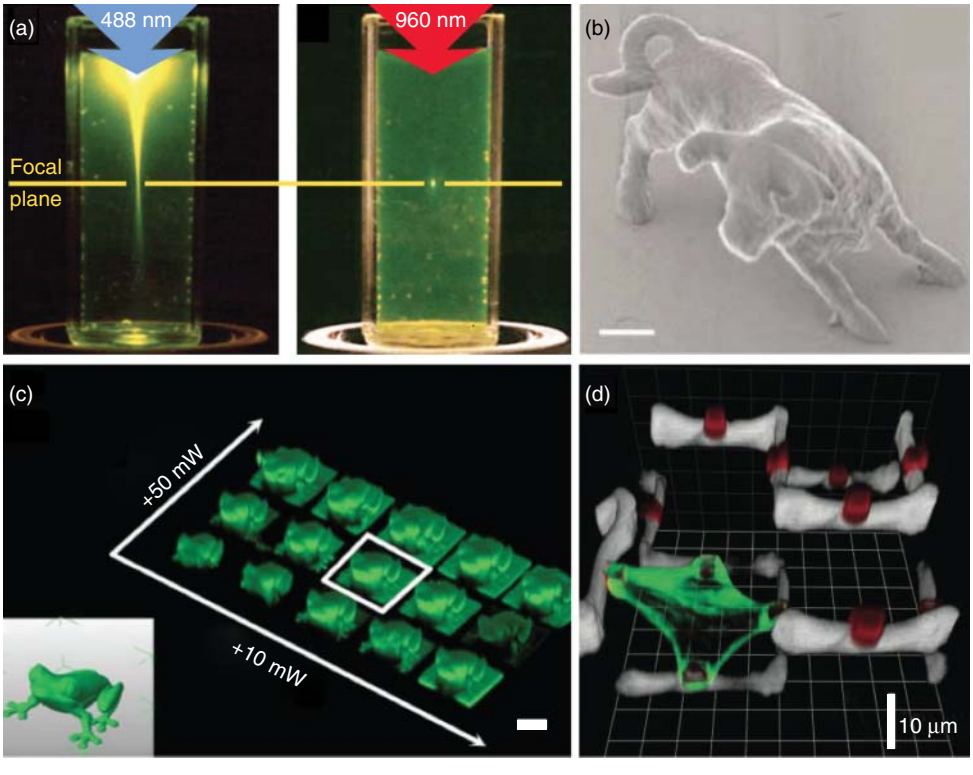

Figure 8.1 Materials fabricated by MPL photopolymerization. (a) The nonlinear nature of multiphoton excitation results in a decreased excitation volume (960 nm) compared to single photon excitation (488 nm). (Zipfel 2003 [30]. Reproduced with permission of Nature Publishing Group.) (b) A microbull fabricated by two-photon photopolymerization. Scale bar = 2 µm. (Kawata 2001 [31]. Reproduced with permission of Nature Publishing Group.) (c) Hydrogel frogs patterned with MPL. Scale bar = 60 µm. (Li 2013 [32]. Reproduced with permission of Royal Society of Chemistry.) (d) Primary chicken fibroblast interacting with composite microfabricated cell scaffold. Scale bar = 10 µm. (Klein 2011 [33]. Reproduced with permission of Wiley.)

cellular structures as biomaterials or photonic crystals [39, 40]. In principle, the technique is amenable to any rendering accessible through traditional computer-assisted drawing (CAD) software, and this has been demonstrated through the fabrication of many complex objects, such as a bull, frogs, and composite culture scaffolds (Figure 8.1) [31–33].

The main advantage of MPL over traditional LSL is the greatly increased *z*-resolution afforded because the axial dispersion of the point spread function is significantly decreased compared to single-photon excitation [30]. Additionally, the use of IR or near-IR light enables increased penetration depth, as these wavelengths are minimally absorbed and scatter less in most media, including biological samples [30]. These advantages afford true 3D patterning at size scales commensurate with the focal volume of the multiphoton laser (<1 fl or 1 μm^3), which conveniently accesses subcellular length scales pertinent to cell and tissue biology.

While MPL improves the voxel resolution for photopolymerized biomaterials and hydrogels, practical constraints of the technology still exist. MPL remains limited in total thickness without using advanced stages and by the throughput of fabrication, which remains low for high-feature-content, millimeter-sized objects. Additionally, the available photoinitiator toolbox, those photoinitiators that are amenable to multiphoton excitation, should be improved. Advances in computational quantum chemistry are beginning to elucidate novel photoinitiators that are susceptible to multiphoton excitation and cleavage to generate initiating radicals [41]. Excitingly, water-soluble initiators with favorable two-photon cross sections are under development for biological applications [32].

8.3 MPL Equipment for Biomaterial Fabrication

A complete discussion of the equipment and techniques for MPL can be found in Part II. For the polymer or biomaterial scientist, the user will likely employ either commercial LSMs or home-built setups. In fact, the main limitations are the requirement for a multiphoton laser source (e.g., a femtosecond pulsed Ti:sapphire laser), a suitable light path with focusing optics, a high-fidelity *xyz* stage, and software to raster the laser focal volume through the sample, or vice versa. All of these requirements are met with commercial MPMs (e.g., Zeiss 710 NLO, Nikon A1R MP+, Olympus Fluoview FVMPE series) designed primarily for imaging biological samples. Such systems are adapted for writing instead of reading by rastering the focal volume through a precursor solution within defined regions of interest (ROIs) that define the shape to be polymerized. Advances in CAD-supported ROI software are facilitating easy translation of arbitrary structures into 3D photopolymerized materials using commercial microscopes. Additionally, to achieve high-resolution patterning with high fidelity, MPL equipment requires an automated [42] stage with independent *x*-, *y*-, and *z*-dimension resolution at the sub-micrometer scale.

8.4
Chemistry for MPL Photopolymerizations

The major requirements for photopolymerizations are a precursor solution containing a photoinitiator and functional monomer or macromers as well as a light source for initiation. In this section, the focus will be on the chemistries and mechanisms for photopolymerization of biomaterials and hydrogels via MPL.

8.4.1
Photopolymerization

Photopolymerizations comprise a particularly attractive mechanism for the fabrication of biomaterials via MPL, as they rapidly convert a liquid precursor solution into a solid material only within the regions of irradiation. This allows easy removal of the unwanted material and recovery of the desired microstructured biomaterial. The initial step in a radical-mediated photopolymerization reaction is photoinitiation. Photoinitiation occurs when a photoinitiator molecule (PI) absorbs a photon of light – or in the case of MPL multiple photons nearly simultaneously – and enters an excited state. The excited-state photoinitiator (PI*) is capable of following one of two pathways: (i) dissociate directly into one or multiple primary radicals (Type I PI), or (ii) undergo a bimolecular reaction wherein the excited PI reacts with a second molecule to generate free radicals (Type II PI) [43]. The rate of initiation, R_i, for a Type I PI undergoing two photon photoinitiation from a typical pulsed laser is given by [44, 45]

$$R_i = 2 \cdot 1.17 \delta_u \Phi_u \frac{T}{\tau_p} \left(\frac{\lambda}{\pi h c w_{xy}^2} \right)^2 P_{avg}^2 \mathrm{VF[PI]} \tag{8.1}$$

where $\delta_u \Phi_u$ is the two-photon cross section (generally a function of λ), T is the period of the laser pulses, τ_p is the duration of the laser pulses, λ is the wavelength of the laser light, h is Planck's constant, c is the speed of light, w_{xy} is the lateral focal radius of the laser, P_{avg} is the average laser power, VF is a volume factor (taken as 0.63 for an axial cylinder), and [PI] is the local concentration of the photoinitiator. The prefactor of 2 assumes that two radicals are generated for each dissociated photoinitiator molecule. Similar rate expressions can be derived for other multiphoton initiation processes. Most single-photon photopolymerizations are hindered by light attenuation, which creates a spatial gradient in light intensity, as well as out-of-plane initiation. Owing to the limited scattering and absorption of IR light in most media, the light intensity or average power is assumed uniform over the spatial domain of the polymerization. Quantifying the rate of initiation is critical, as the rate of initiation affects the rate of polymerization and, thus, the final material properties. As shown in Eq. (8.1), the rate of initiation can be controlled by tailoring the PI concentration, selecting a PI with a favorable two-photon cross section, tuning the wavelength of light, or adjusting the laser power. As opposed to single-photon initiation, the rate of two-photon initiation varies quadratically with the input laser power.

Once radicals are generated within the precursor solution, they begin to propagate through the functional groups of the monomers or macromers, assuming the radicals do not immediately recombine within the solvent cage. In principle, polymerization reactions proceed through a chain or step-growth mechanism [43]. In a classic, radical-initiated, step-growth (or condensation) polymerization, a radical activates a functional group (such as a thiol) on one of the surrounding monomers, which then adds to another functional group (such as a vinyl) on a second monomer while the radical transfers to another functional group in solution. In this manner, dimers are formed. Dimers can then react with monomers or other dimers to form trimers or tetramers, which sequentially build up in mass in a stepwise manner. In contrast, a classic, chain-growth (or addition) radical-initiated polymerization proceeds when a radical activates a functional group (such as a (meth)acrylate) on one of the surrounding monomers, which then activates and adds to another monomer in solution. This proceeds iteratively through monomer addition to form long chains of monomers from each initiation event. In either case, polymerization results in high molecular weight species that form an entangled polymeric solid or, when multifunctional monomers/macromers are in solution, a crosslinked polymer network. During this process, radicals can also terminate as opposed to initiate or propagate the reaction, which decreases the concentration of radicals in solution and affects the kinetic rate of polymerization. Termination can occur through several mechanisms, including bimolecular combination between two active chain ends or an active chain end and an initiating radical; disproportionation, in which a hydrogen atom is abstracted from one active chain by another; interaction with inhibitors such as oxygen; and chain transfer to nonpropagating species [43]. The kinetic rate of polymerization, R_p, for chain growth polymerizations accounts for both propagation and termination as follows [43]:

$$R_p = k_p[M]\left(\frac{R_i}{2k_t}\right)^{1/2} \tag{8.2}$$

where k_p is the rate constant for propagation, $[M]$ is the macromer functional group concentration, and k_t is the rate constant for termination. This chapter is focused on the formation of crosslinked networks and hydrogels. In these systems, k_p and k_t vary as a function of macromer conversion or polymerization time on account of the changes in the diffusion constants of the reacting species caused by the reaction of the precursor solution [46]. At early macromer conversion, the viscosity of the precursor solution increases, limiting the radical diffusion rate and, thus, the rate constant for termination k_t. The viscosity-mediated decrease in k_t leads to an increase in the rate of polymerization termed *autoacceleration*. As the macromer conversion increases and a crosslinked network begins to form, the macromer functional groups also become diffusion-limited, causing a decrease in k_p and the an overall decrease in R_p. This phenomenon is referred to as *autodeceleration* and, combined with a consumption of functional groups, leads to a cessation of the polymerization.

The kinetics of photopolymerization reactions are more completely described elsewhere with extra considerations for polymer networks and hydrogels [6, 17, 47, 48]. In general, by accounting for multiphoton photoinitiation kinetics, these same principles can be applied to MPL photopolymerizations. Understanding the kinetics of the photopolymerization is critical in the fabrication of networks and hydrogels to be used as biomaterials, as the extent of reaction affects the final material properties and biological function. For instance, in hydrogels, the crosslinking density influences not only the mechanical properties of the gel but also the water swelling ratio, the transport of nutrients and waste, as well as the degradation kinetics [49].

8.4.2 Photoinitiator Selection

PIs are organic compounds capable of converting absorbed light into active chemical species that can initiate polymerization [50]. Depending on the chemical makeup of the parent PI, the active species can be cationic, anionic, or radical in nature, thereby enabling all types of chain-growth and step-growth polymerizations to be controlled with light. As both cationic and anionic polymerization methods are highly moisture-sensitive, polymerizations within a biological context are performed nearly exclusively by free-radical methodologies. Radical PI systems can contain one or more components. Type I initiators operate independently and are typically based on the heterolytic cleavage of aromatic ketones or disilanes. Type II PIs do not themselves cleave, but instead work in conjunction with a co-initiating species (usually non-photoactive) to induce polymerization, often through hydrogen abstraction. As greater energy is associated with bond photolysis than molecular excitation, type I PIs are largely confined to UV light sources ($\lambda < 400$ nm), while type II PIs can be initiated with light extending well into the visible range ($\lambda < 600$ nm).

A complete description of photoinitiators amenable to MPL is presented in Chapter 6. In general, this class of photoinitiators – those that can be activated by multiphoton excitation – can be applied to fabricate biomaterials; however, certain constraints apply. In all biomaterials, the constituent components as well as the associated degradation products or leachants must be minimally biocompatible. In this context, this means that cells, tissue, and organisms must tolerate the photoinitiators and their cleavage products post fabrication. Additional constraints apply for hydrogels, particularly those employed for cell encapsulation. Radical polymerization must operate under stringent physiological conditions if the interest is in performing the polymerization in the presence of live cells: body temperature (37 °C), pH (7.4), oxygen content (5%), and buffering salts must all be accommodated. Additionally, biological conditions further necessitate an aqueous environment, dramatically limiting the selection of available PIs. As most PIs absorb light through the presence of conjugated aromatic moieties, the significant hydrophobicity of these same functionalities leads to poor water solubility. If a candidate PI is able to meet these restrictive conditions, the small molecule

need also be non-cytotoxic at the concentrations used to initiate photopolymerization, as well as in the range of light in which they operate. Typically, light with $\lambda \geq 365$ nm is considered appropriate for use in biological systems [51]. These wavelengths usually have enough energy to initiate polymerization, but not so much as to denature proteins and damage cellular DNA (known to occur rapidly at $\lambda = 254$ nm) [52, 53].

Despite the restrictive requirements posed in performing photopolymerization in the presence of live cells, several key PIs have been identified as invaluable for such tasks (Figure 8.2). Irgacure® 2959 [2-hydroxy-1-(4-(2-hydroxyethoxy)phenyl)-2-methylpropan-1-one] has perhaps the most widespread use, and decomposes under UV light ($\lambda = 365$ nm) to form both an acetone ketyl and a substituted benzoyl radical (Figure 8.2a) [51]. Though these active radicals initiate chain polymerization rapidly in aqueous systems, the parent PI suffers from poor water solubility (~1 wt%, ~50 mM). This, coupled with relatively low activity at cytocompatible wavelengths of light, dramatically limits the initiation rates [54]. More recently, lithium phenyl-2,4,6-trimethylbenzoylphosphinate (LAP) has been rediscovered as a water-soluble (~8.5 wt%, ~300 mM) type I PI that exhibits high molar absorptivity in the range $300 < \lambda < 400$ nm (Figure 8.2b) [55, 56]. Upon exposure to UV light, LAP dissociates into a 2,4,6-trimethylbenzoyl

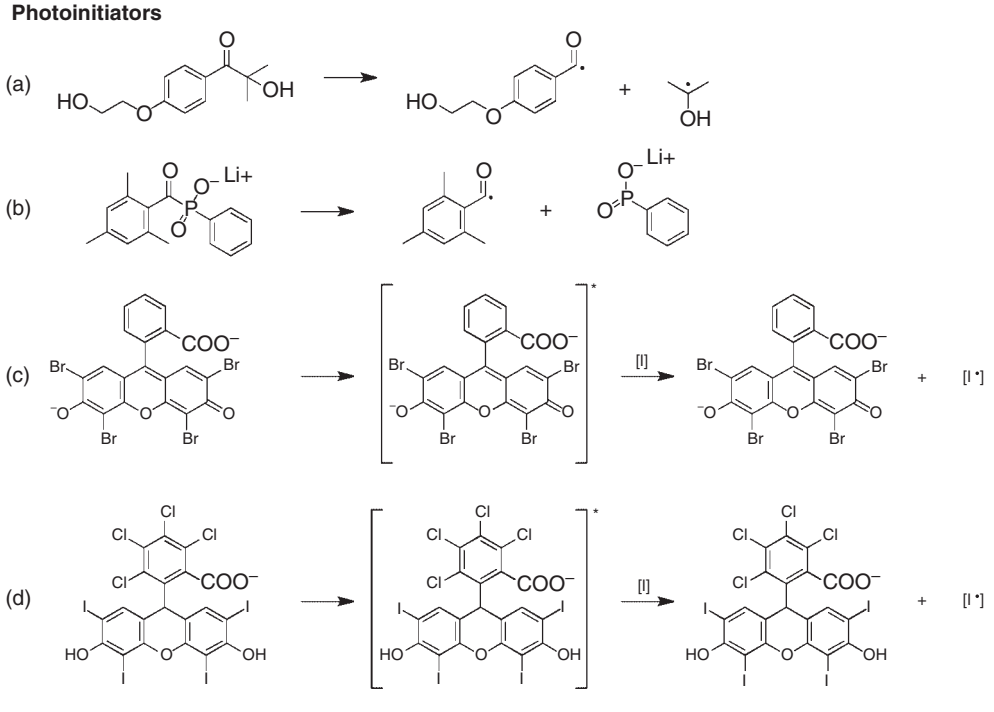

Figure 8.2 A selection of type I and type II photoinitiators amenable to MPL that have been employed in the presence of live cells. (a) Irgacure 2959. (b) Lithium phenyl-2,4,6-trimethylbenzoylphosphinate (LAP). (c) Eosin Y. (d) Rose Bengal.

and a phosphonyl radical, both of which can initiate polymerization efficiently in cellular systems. Though the LAP PI is not commercially available, its two-step synthesis is straightforward and nearly quantitative [56].

Several type II PIs have also been utilized for photopolymerization in the presence of cells. These most commonly used include rose Bengal, eosin Y (Figure 8.2c,d), and camphorquinone [57]. When exposed to light, these compounds get excited to a triplet state, which reacts with a hydrogen-donating co-initiator (e.g., an amine or thiol containing molecule) to produce an initiating free radical. Despite their wide usage, as well as their unique ability to perform effectively in the visible range, the photokinetics of type II systems are less understood than their type I counterparts [58].

8.4.3 Photopolymer Chemistries

8.4.3.1 Macromer Chemistries

The photopolymerization precursor solution also requires the selection of appropriate macromer chemistries for material fabrication. The macromer selection can be approached in two stages: (i) deciding on a backbone chemistry, and (ii) choosing a linking chemistry for network formation. Fortunately, single-photon photopolymerization of biomaterials and hydrogels has been employed extensively over the last few decades and has identified a broad range of backbone and linking chemistries for the formation of biocompatible polymer networks and hydrogels. In principle, the same toolbox can be adapted to MPL fabrication given that the photoinitiator and light source chosen provide a sufficient source of radicals to drive polymerization. This section serves to introduce a subset of the available toolboxes even though the specific chemistries have not yet been explicitly utilized with MPL. A brief overview of MPL biomaterials is presented in Section 8.5.

Typical non-hydrogel photopolymerized biomaterials employ a polymeric resin-like precursor solution that is composed of functional monomers, oligomers, or macromers and a suitable photoinitiator that can be polymerized rapidly into a solid. Common resins that have been applied to fabricate photopolymerized biomaterials include (meth)acrylates, epoxides, urethanes, styrenes, *n*-vinylpyrrolidone, and other vinylic small molecules [57]. In these systems, polymerization induces the formation of high molecular weight, insoluble, and entangled polymers that comprise a solid material. In parallel, functional oligomers or macromers are also used to make biomaterial based on non-hydrophilic backbone polymers. Such hydrophobic backbone chemistries include esters [59], carbamates [60], and carbonates [61] that are end-functionalized with polymerizable moieties such as vinyl groups or complementary thiol and ene functionalities [62]. Included in this class of materials are the biophotopolymers that have been used to fabricate microstructured biomaterials using MPL [63].

For the fabrication of hydrogels, the main constraint is that the backbone chemistry be hydrophilic. Decades of research on the use of hydrogels as biomaterials have provided a wealth of information on backbone chemistries

for this application, all of which equally applies to MPL hydrogels [64]. In general, hydrophilic polymers can be segregated into two main classes: synthetic polymers and natural polymers. Synthetic polymers for hydrogel synthesis include poly(ethylene glycol) (PEG), poly(vinyl alcohol) (PVA), poly(acrylic acid) (PAA), and poly(2-hydroxyethylmethacrylate) (PHEMA) [65]. Of these, PEG or poly(ethylene oxide) (PEO) have found prolific use on account of their non-fouling behavior and ability to mimic the elasticity and transport of native tissue. Natural polymers for hydrogel fabrication include alginate, collagen/gelatin, hyaluronic acid, fibrin, chondroitin sulfate, and cellulose derivatives [66]. In either case, synthetic or natural, the polymers can be functionalized with a variety of polymerizable moieties (such as (meth)acrylates, (meth)acrylamides, or thiol–ene pairs) to render the backbone polymers amenable to photopolymerization. Once crosslinked via photopolymerization, the insoluble polymer network imbibes water and swells, resulting in a functional hydrogel [66].

In each material class – resins, networks, or hydrogels – the backbone chemistry often defines the bulk chemical properties of the material, which influence protein fouling, biocompatibility, cell adhesion, degradation, and mechanical integrity [12]. The linking chemistry defines the kinetics of formation, the microarchitecture, and crosslinking density [49]. Given the large toolbox, the orthogonal selection of backbone chemistry and linking chemistry spans a large parameter space of material properties. Additional information on the specific linking chemistries amenable to photopolymerization is provided in the following section.

8.4.3.2 Photochemical Polymerization and Degradation

Hundreds of photo-mediated reactions have been utilized for both the formation and degradation of polymers. In this section, we seek to highlight the diverse subset of these chemistries that have been performed within a biological context. Additive photoreactions are classified according to their utilization of PIs, photocaged reactive groups, or nonspecific radicals. Strategies that employ photolabile linkers to achieve subtractive degradation, as well as those offering reversible photofunctionalization, are also described. All discussed reactions are illustrated in Figures 8.3–8.7.

Initiator-Mediated Photopolymerization To date, the majority of photopolymerization reactions are initiator-mediated. As PI identity can be selected independently from that of the reactive species, reactions utilizing PIs offer increased tunability over initiation wavelengths, solvent composition, and reaction kinetics. Some common PI-mediated polymerization mechanisms that have been performed for biomaterial synthesis include vinyl chain polymerization, thiol–ene and thiol–yne reactions, and the photo-inducible copper-catalyzed azide–alkyne cycloaddition (pCuAAC) (shown in Figure 8.3).

Vinyl chain polymerization

Perhaps the most common photopolymerization reaction, namely radical chain polymerization of vinyl monomers (i.e., those that contain

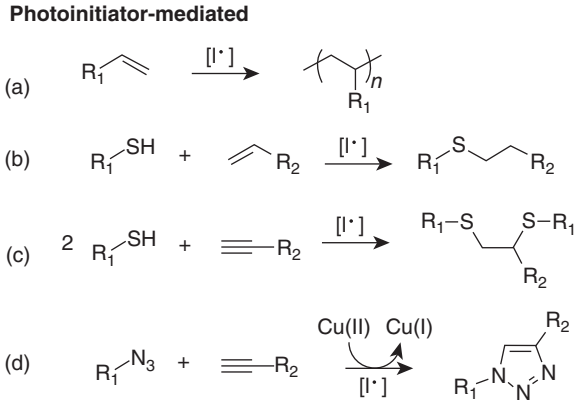

Figure 8.3 Photoinitiator-mediated polymerization reactions used for biomaterial synthesis and modification include (a) vinyl chain polymerization, (b) thiol–ene, (c) thiol–yne reactions, and (d) the photoinducible copper-catalyzed azide–alkyne cycloaddition.

carbon–carbon double bonds), occurs through a series of initiation, propagation, and termination steps [43]. During initiation, free-radical-containing initiator fragments attack the pair of π electrons on the vinyl monomer. This forms a bond between the initiator species and the monomer while simultaneously generating a new free radical at the chain end. The free radical on the growing polymer chains then reacts in a similar manner with additional monomer, iteratively increasing polymer length by one repeat unit during repeating steps of propagation. Polymer growth can be halted through a variety of different termination events, each of which destroys the active radical species. In a biological context, these can include reactions with oxygen, cellular proteins, DNA, and polysaccharides, making polymerizations in the presence of living cells more challenging [67]. Monomers are most typically substituted acrylates and methacrylates, where changes in substituent structure give rise to materials with different properties (e.g., temperature responsiveness, water content, compliance). These systems have been used extensively for the formation and modification of biomaterials and hydrogels [7, 26, 68].

Thiol–ene photoaddition

In this step-growth polymerization reaction between thiols and alkenes [62, 69], an active photoinitiator first abstracts a thiolic hydrogen to form a thiyl radical. The thiyl then propagates across the ene functional group to form a carbon-centered radical, which then abstracts a hydrogen from another thiol. Alternating steps of propagation and chain transfer give rise to a 1 : 1 addition of thiol- and ene-containing monomers, provided that the ene functionality exhibits no homopolymerization. Thiol–ene reactions proceed most quickly for electron-rich (e.g., vinyl ethers) or strained (e.g., norbornene) monomers. Notably, thiol–ene polymerizations work well with type II initiators, as the monomeric thiol can also serve as the

hydrogen-donating co-initiator [70]. The reaction has been exploited for the formation of biomaterials derived from synthetic [71, 72] and natural polymers [73, 74], the formation of cyclic peptides [75], as well as in the biochemical decoration of ene-containing hydrogel networks [70, 76–78].

Thiol–yne photoaddition

Similar to the thiol–ene reaction, the thiol–yne reaction proceeds through the addition of an initiator-generated thiyl radical to an alkene [79]. The resulting carbon-centered radical abstracts a hydrogen from an additional thiol, thereby generating a vinyl sulfide intermediate and regenerating the sulfanyl radical. The monosubstituted vinyl sulfide can undergo further reaction with an additional thiyl radical via a thiol–ene reaction. The net result is the double addition of two thiols to a single alkyne to generate a dithioether. The uniqueness of this double reaction allows the facile creation of dendrimers [80, 81], the rapid generation of multivalent peptides [75], and crosslinked hydrogel materials to be formed from monomers containing just a single yne group [82, 83].

Photo-inducible copper-catalyzed azide-alkyne cycloaddition (pCuAAC)

The azide–alkyne Huisgen cycloaddition represents a 1,3-dipolar cycloaddition between an azide and a terminal or internal alkyne to give a triazole linkage. Though this reaction can be performed in the absence of a catalyst at high temperatures, pressures, or through the utilization of strained alkynes, the reaction kinetics can be increased dramatically through catalysis with Cu(I) (by a factor of $\sim 10^7$) [84–86]. In recent work by the Bowman group, photogenerated initiator fragments were shown to reduce Cu(II) to Cu(I) transiently, thereby providing photochemical control over the copper-catalyzed azide–alkyne cycloaddition (CuAAC) [87, 88]. This reaction has been utilized for photopolymerization/functionalization of hydrogel materials.

Photocage-Mediated Photoconjugation Photocages function as molecular gatekeepers for the regulation of chemical reactions. When intact, these compounds serve to block the reactivity of two species through physical masking. Upon photolysis, the reactive functional group is liberated, thereby permitting species reaction and photoconjugation to occur. To date, photocage-based regulation of the strain-promoted azide–alkyne cycloadditon (SPAAC), oxime ligation, Michael-type addition, and enzymatic crosslinking have proven the most promising for biological studies, and they are shown in Figure 8.4.

Strain-promoted azide–alkyne cycloadditon (SPAAC)

A strain-promoted reaction between cyclooctynes and azides has been established by the Bertozzi group as an effective means to perform traditional Huisgen cycloadditions rapidly without the need for a cytotoxic copper catalyst [89, 90]. The phototriggerability of the reaction has been demonstrated by the Popik group, who masked the triple bond of a dibenzocyclooctyne as cyclopropenone [91]. Upon exposure to UV light

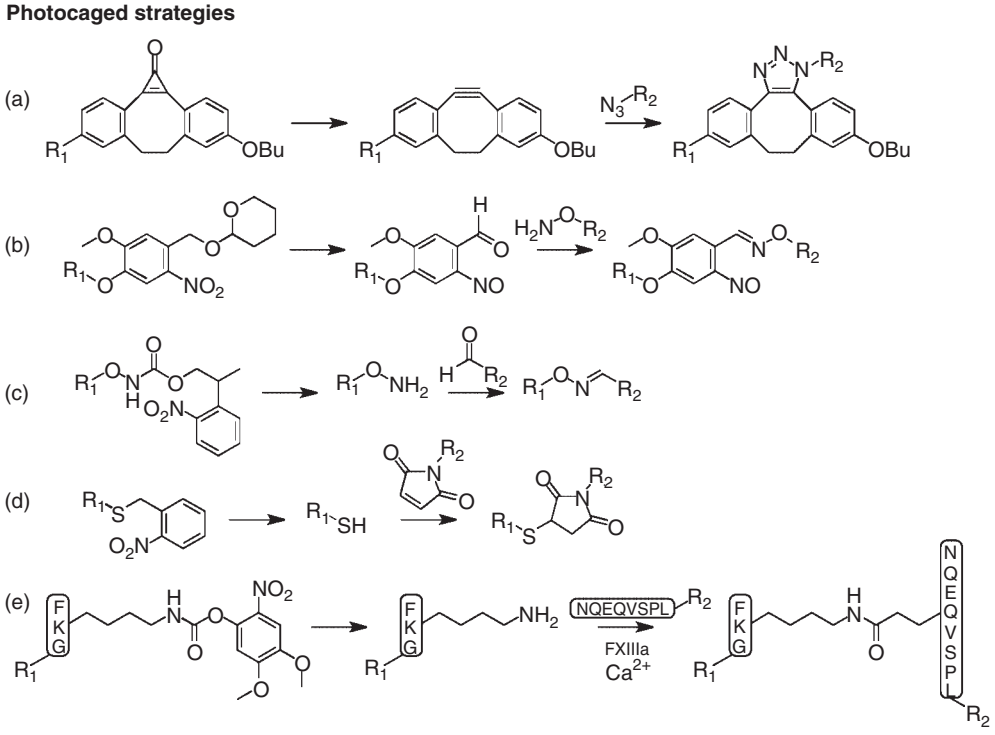

Figure 8.4 Photocaged regulation of (a) strain-promoted azide–alkyne cycloadditon, (b,c) oxime ligation, (d) Michael-type addition, and (e) factor XIII enzymatic crosslinking have proven the most promising conjugation reactions for synthesis and modification of biopolymer systems.

($\lambda = 350$ nm), cyclopropenone undergoes a photochemical decarbonylation to yield quantitatively the strained alkyne, which is then able to react with azides. This reaction has been utilized for the photochemical labeling of cellular glycoproteins and surfaces [92–94].

Oxime ligation

The condensation reaction of alkoxyamines with aldehydes or ketones yields oxime linkages that are both formed and stable under physiological conditions. Photocontrol over oxime ligation has been independently effected through strategies that cage each of the two reactive species. Barner-Kowollik and coworkers demonstrated that the photocleavage ($\lambda = 365$ nm) of *o*-nitrobenzyl derivatives, which typically leads to the generation of a nitrosobenzaldehyde, can be exploited to give spatiotemporal control over aldehyde formation [95]. The photogenerated aldehydes then react with hydroxylamines to form oxime linkages. This reaction sequence has been utilized to pattern fluorescent peptides onto reactive surfaces. In an alternative strategy developed by Dumy, the alkoxyamine has been photocaged with a 2-(2-nitrophenyl)propyloxycarbonyl (NPPOC)

group [96]. Under brief irradiation with UV light ($\lambda = 365$ nm), NPPOC undergoes irreversible cleavage to yield CO_2, a styrene byproduct, and the reactive alkoxyamine. This reaction has been exploited for the conjugation of small molecules and peptides to glass surfaces [96–98].

Michael-type addition

The Michael-type addition of nucleophiles to electron-deficient alkenes represents one of the most common reactions in organic chemistry. Though a variety of nucleophilic Michael donors/acceptors exist, thiol–maleimide and amine–acrylate represent important variants, both of which have been controlled with light. The Shoichet group has demonstrated that thiols can be masked with both 2-nitrobenzyl- and coumarin-based photocages, and will subsequently react with maleimides upon irradiation [99–101]. Moreover, the Bowman group has demonstrated that NPPOC can serve as a photolabile protecting group for primary amines, which enables thiol-Michael additions with acrylates to be phototriggered [102]. These chemistries have been used to form hydrogel biomaterials [103] as well as to guide 3D cell function through immobilized biomolecules [99, 101].

Light-activated enzymatic crosslinking reaction

A strategy for light-activated enzymatic crosslinking utilizing factor XIII (FXIIIa) has been recently introduced by both the Lutolf and Segura groups [104, 105]. FXIIIa represents a transglutaminase enzyme that catalyzes covalent amide bond formation between the ε-amino group on a lysine (K) and the γ-carboxamide residue of glutamine (Q) of FKG and NQEQVSPL peptides. When the critical lysine residue is caged with an *o*-nitrobenzyl functional group, FXIIIa is unable to crosslink the two independent peptides. After cage photolysis, however, the two peptides are rapidly joined through FXIIIa-mediated chemoenzymatic ligation. These approaches have been utilized to pattern short peptides and synthetic proteins into hydrogels and used to guide cellular growth within a material.

Nonspecific Photoconjugation Several photoreactive groups have been developed that couple nonspecifically with target molecules upon activation with UV light exposure. The indiscriminant nature by which these moieties couple to local molecules enables rapid addition as well as covalent linkage between biomacromolecules that are in close proximity in 3D space. Aryl azides, diazirines, and benzophenones represent the most common functionalities for nonspecific photoconjugation and are highlighted in Figure 8.5.

Aryl azides

Perhaps the most popular of the nonspecific photoconjugation reactions, aryl azides form short-lived nitrenes upon exposure to UV light ($250 < \lambda < 350$ nm) [106]. These intermediate nitrenes can either insert nonspecifically into carbon–hydrogen bonds, or rearrange to form ring-expanded dehydroazepines prior to addition reaction with nucleophiles or carbon–hydrogen bonds. Photocrosslinking of aryl azides has

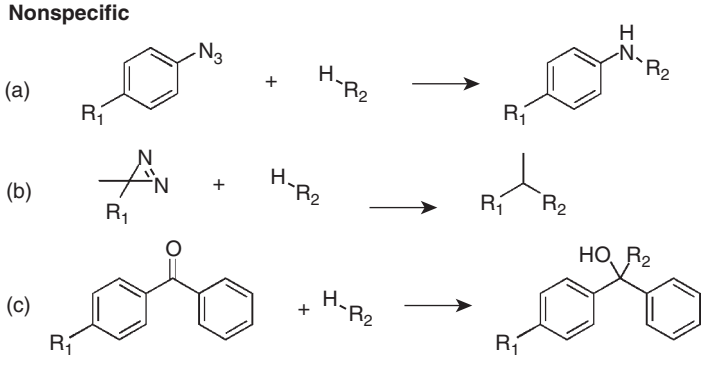

Figure 8.5 A variety of nonspecific chemical conjugation reactions have been utilized for photo-mediated biomaterial synthesis including those involving (a) aryl azides, (b) diazirines, and (c) benzophenones.

been extremely beneficial in capturing and probing protein interactions [107, 108], patterning cell-adhesive proteins to surfaces [109], and identifying peptide–receptor binding domains [110].

Diazirine

In the presence of UV light ($330 < \lambda < 370$ nm), diazirine compounds undergo photolysis to form a highly reactive carbine intermediate while simultaneously giving off nitrogen gas [111]. The resulting carbine yields efficient insertion into hydrogen–carbon and hydrogen–nitrogen bonds, as well as with unsaturated bonds within target molecules. These molecules have been useful in studying the effects of protein interactions in cells [112, 113], crosslinking protein-based hydrogels [114], and identifying targets of membrane receptors [115, 116].

Benzophenone

When exposed to UV light, benzophenone photolysis yields a highly reactive triplet-state ketone intermediate [117]. The energized electron of this activated benzophenone can insert into hydrogen–carbon bonds within the target molecules. Interestingly, the activated intermediate relaxes to yield the original benzophenone moiety when no covalent linkage is formed. The resulting potential for multiple activation gives rise to higher overall yields of photocrosslinking than with phenyl azide and diazirine crosslinkers. Though benzophenone as a photoaffinity tag permeates much of biochemistry [118], the molecule has also been used to attach peptides and polymer films to solid surfaces [119–121].

Light-Mediated Degradation Though the majority of photochemical reactions result in the formation of covalent bonds, there is growing interest in photoactive linkers that undergo cleavage in response to photonic irradiation. When incorporated into the backbone of polymeric species, these moieties provide a tunable handle for network depolymerization. Here, we highlight (Figure 8.6)

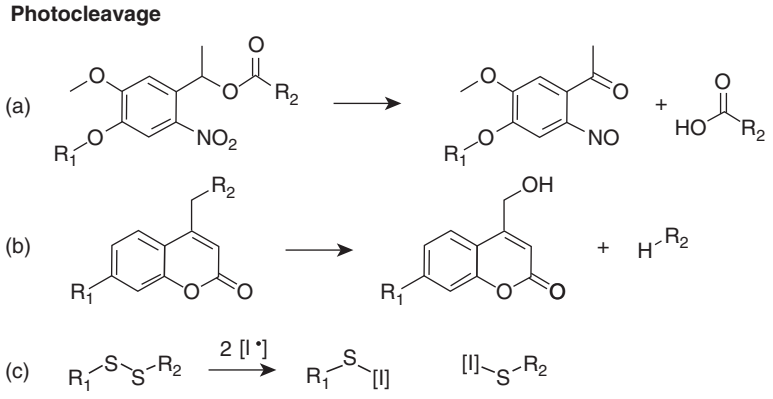

Figure 8.6 Photolabile linkages including (a) *o*-nitrobenzyl esters, (b) coumarins, and (c) disulfide-containing compounds can be photochemically cleaved under physiological conditions using MPL, enabling on-demand biopolymer depolymerization.

o-nitrobenzyl esters, coumarins, and disulfide-containing compounds as photocleavable species that can be controlled in a biological context.

o-Nitrobenzyl esters

As one of the most heavily utilized photocleavable linkers, the use of *o*-nitrobenzyl esters for light-based molecular cleavage extends back to the 1970s [122]. Upon photoexcitation, the nitrobenzyl group forms an *aci*-nitro intermediate through either a singlet or triplet excited state. This intermediate further decays to generate both a nitroso and an acid/amide byproduct (depending on parent substitution) [123]. Cleavage rates and photoactive wavelengths ($250 < \lambda < 400$ nm) can be tuned by varying molecular substituents [124–126]. These reactions have been used for the uncaging of proteins [127, 128], controlling cell adhesions [129, 130], photodegrading polymers and biomaterials [70, 131–134], and probing the effects of physical material cues on cell function [135–137].

Coumarin methylester

When irradiated with UV light ($350 < \lambda < 450$ nm), coumarin methylesters undergo heterolytic ester photosolvolysis, leading to the corresponding coumarin methanol and a carboxylic acid [138–140]. Though some coumarins are known to exhibit reversible homodimerization upon exposure to light [141], the methylester variants preferentially undergo photocleavage when irradiated. Coumarins methylesters have been used in the synthesis of caged fluorophores for biological imaging [123], material degradation [142, 143], and drug delivery [144].

Disulfide displacement reactions

Disulfide linkages, formed through the oxidation of thiols, have been demonstrated to be susceptible to radical cleavage by carbon- and phosphorus-center radicals [145, 146]. As such, disulfide linkages can be

selectively displaced with radical species, including initiator fragments generated from exposure of PIs to light. Anseth *et al.* demonstrated that polymer-based hydrogels crosslinked with disulfide linkages could undergo complete and rapid photodegradation when exposed to sufficient amount of initiator radicals [147].

Reversible Photoconjugation Though the majority of the utilized chemistries have focused on either photomediated bond formation or cleavage, great interest lies in the development of photochemical processes that can be controlled in a fully reversible manner. Two of the most promising systems to date that can be used in a biological context include the reversible dimerization of anthracene and the allyl sulfide addition–fragmentation chain-transfer reaction. Both examples are shown in Figure 8.7.

Anthracene dimerization

Anthracene is capable of absorbing light over a broad spectrum ($250 < \lambda < 400$ nm), most frequently yielding a fluorescence emission ($390 < \lambda < 450$ nm). However, when anthracene is exposed to UV light ($\lambda = 360$ nm), a dimerization reaction can also occur [148, 149]. Interestingly, this reaction can be partially reversed when the dimers are illuminated with higher intensity light ($260 < \lambda < 280$ nm) [150]. These sequential reactions have been used for photocontrolled drug delivery [151], biomaterial formation and degradation [152, 153], and nanoparticle manipulation [154].

Allyl sulfide addition–fragmentation chain transfer

Allyl sulfides, typically employed as the transfer agent in reversible addition–fragmentation chain transfer (RAFT) polymerizations [155],

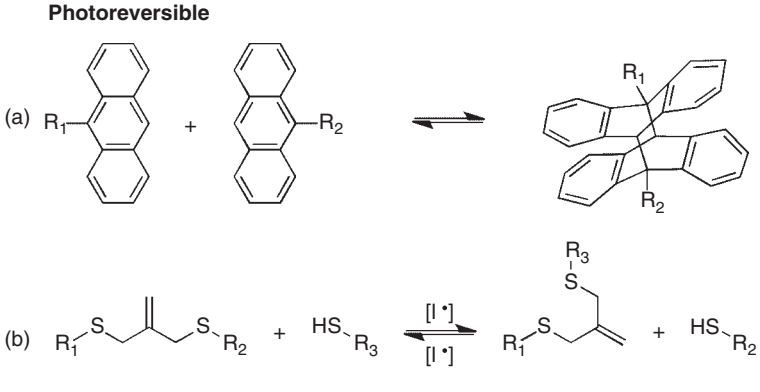

Figure 8.7 Reversible photochemistries open up the door to dynamic spatiotemporal control over biopolymer addition and degradation, as well as material formation and functionalization. The most promising examples to date include (a) the reversible dimerization of anthracene, and (b) the allyl sulfide addition–fragmentation chain transfer reaction.

can undergo reversible exchange with thiol-containing molecules [156, 157]. Here, a thiyl radical attacks the carbon–carbon π bond of the allyl sulfide, resulting in an unstable trifunctional intermediate. The instability of this intermediate leads to a β-cleavage, which results in the addition of the initial attacking species while regenerating a new double bond. As the regenerated double bond is susceptible to attack by other thiyl radicals, the linkage is said to be "living." Initial thiyl radicals are readily generated using PIs in the presence of light. Photoinitiated RAFT has been used extensively for the synthesis of biopolymers [158], to induce plasticity in crosslinked networks [159], to create self-healing materials [160], and to reversibly decorate hydrogel networks with synthetic peptides [161].

8.5 Biomaterial Fabrication

Initial work with MPL photopolymerization focused on the development on non-biological materials [162]. Polymerizable resins (or negative-tone photoresists) have been employed in MPL material fabrication, often starting as viscous liquids or amorphous solids. These systems can be easily transformed into complex structures such as interconnected microchannels [163], interlocking chains [164], or renditions of the Venus de Milo [165]. The field of photonics was an early adopter of the MPL paradigm for application-based materials. MPL polymerization has been employed to generate functional waveguides [166], interferometers [167], microlenses [168], and microlasers [169]. Based on the ability to generate features on the sub-micrometer scale, the community has adapted these approaches to generate photonic crystals with stop bands in the visible range. In other approaches, MPL polymerization has been exploited to generate active mechanical devices including springs, cantilevers, and nanorotors [162]. Based on the successful implementation of these techniques, researchers began exploring the use of polymer precursors for the fabrication of structured materials for biological applications.

Cells reside in the body within a complex, dynamic, and highly structured ECM, which choreographs cell fate through bidirectional cell–ECM interactions. Many spatiotemporal signals are integrated by the cell to inform output cellular functions including adhesion, proliferation, differentiation, migration, and tissue morphogenesis [170]. The specific mechanisms through which the ECM directs cell function is still not fully understood. Biomaterial strategies provide attractive platforms to dissect complex and dynamic cell–ECM communication as well as to engineer scaffolds to leverage these cues for regenerative medicine applications [15, 171]. Within this paradigm, photopolymerization reactions via MPL enable precise recapitulation of ECM properties (e.g., biophysical and biochemical signals) in 3D biomaterials with nanometer and micrometer resolution. When exploiting MPL to generate photopolymerized biomaterials, it is important to consider the essential functions and design constraints that apply to materials

for cell culture applications. Minimally, the material should support cell colonization, migration, growth, and differentiation, as well as provide appropriate biophysical and biochemical cues for the specific cell type of interest [172]. In general, two classes of MPL photopolymerized materials have been introduced as biomaterials: biocompatible networks into which cells are introduced post fabrication and hydrogels into which cells can be directly encapsulated.

MPL polymerization affords the generation of highly ordered structures in three dimensions that are biocompatible, degradable, and easily fabricated – all important features for biological implementation. These techniques have been adapted to generate cytocompatible microneedles, biodegradable scaffolds, and ossicular replacement prostheses (Figure 8.8) [173, 174, 177]. To better recapitulate the context of the *in vivo* milieu, MPL has been extended to the fabrication of hydrated polymer networks in the form of hydrogels for cell culture applications [172]. Hydrogels are structurally similar to the native ECM and present an attractive class of materials for tissue engineering and regenerative medicine applications [171]. Specific examples include woodpile lattices, microfabricated porous structures, and vascular trees (Figure 8.8) [42, 175, 178, 179]. Additional work has focused on the manipulation of native proteins for biomedical applications (Figure 8.8) [176, 180–182].

8.6 Biomaterial Modulation

In addition to the synthesis of new biopolymers and biomaterials, photochemical reactions have been utilized to *modify* existing platforms at user-specified points in time and space. Through appropriately developed chemistries, both the physical and chemical material makeup can be altered on demand and with resolution below that of a single mammalian cell. Such high spatiotemporal control over biomaterial composition is critical in capturing the dynamic heterogeneity found in native tissue [15].

Spatiotemporally defined biochemical modulation of existing materials has been performed through both additive or subtractive light-based strategies. In perhaps the most common addition-based chemistry, radical chain polymerization of acrylate-functionalized peptides or proteins has yielded hydrogel materials that promote endothelial cell adhesion as well as enhanced vascular lumen formation through the patterned introduction of the arginylglycylaspartic acid (RGD) binding motif and growth factors such as vascular endothelial growth factor (VEGF) [183]. An alternative reaction between thiols and alkenes has been used to guide changes in cell function within a polymer hydrogel by photopatterning thiol-containing biomolecules into ene-functionalized networks (Figure 8.9a) [184, 185]. Similarly, simultaneous patterning of several proteins can be accomplished by covalently immobilizing protein physical-binding partners (e.g., biotin, barnase) via a photocaged thiol–maleimide reaction [101]. A light-activated enzymatic crosslinking employing factor XIII has also been used

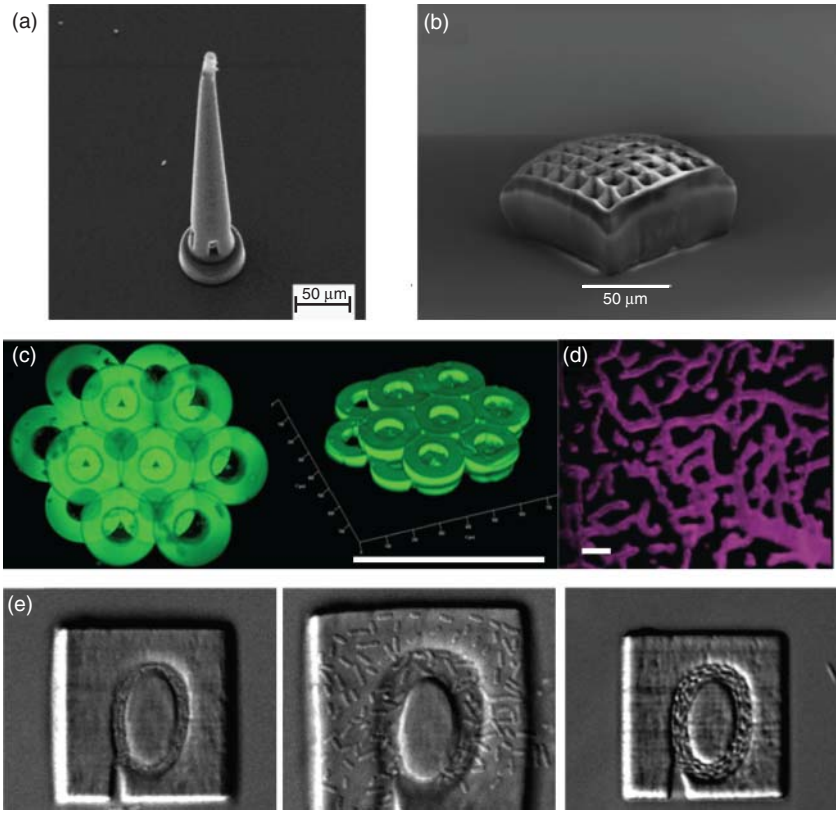

Figure 8.8 Biomaterials fabricated by MPL photopolymerization. (a) Biocompatible microneedles. Scale bar = 50 µm. (Doraiswamy 2006 [173]. Reproduced with permission of Elsevier.) (b) Structured cell culture scaffold. Scale bar = 50 µm (Claeyssens 2009 [174]. Reproduced with permission of American Chemical Society.). (c) Hydrogel cell culture scaffold. Scale bar = 500 µm. (Qin 2013 [175]. Reproduced with permission of Wiley.) (d) Patterned vascular tree. Scale bar = 50 µm. (Culver 2012 [42]. Reproduced with permission of Wiley.) (e) Biochemically responsive protein hydrogel. Scale bar = 5 µm. (Kaehr 2008 [176]. Reproduced with permission of PNAS.)

to photopattern peptides to direct mesenchymal stem cell outgrowth into a 3D material (Figure 8.9b) [104].

Photochemistries have also enabled material biochemical alteration through the selective removal of cues within a material. *o*-Nitrobenzyl (*o*NB) ester cleavage has been utilized for the release of RGD, thereby enhancing chondrogenesis of human mesenchymal stem cells [186]. Additionally, *o*NB cleavage has been used to create functional surfaces to study collective and patterned cell migration [187]. Photocleavage of coumarin derivative dimers has been utilized for a variety of drug delivery applications [141, 188, 189]. While the aforementioned techniques have been used to either introduce or remove biochemical signals, the combination of different photochemical reactions can enable the reversible immobilization of

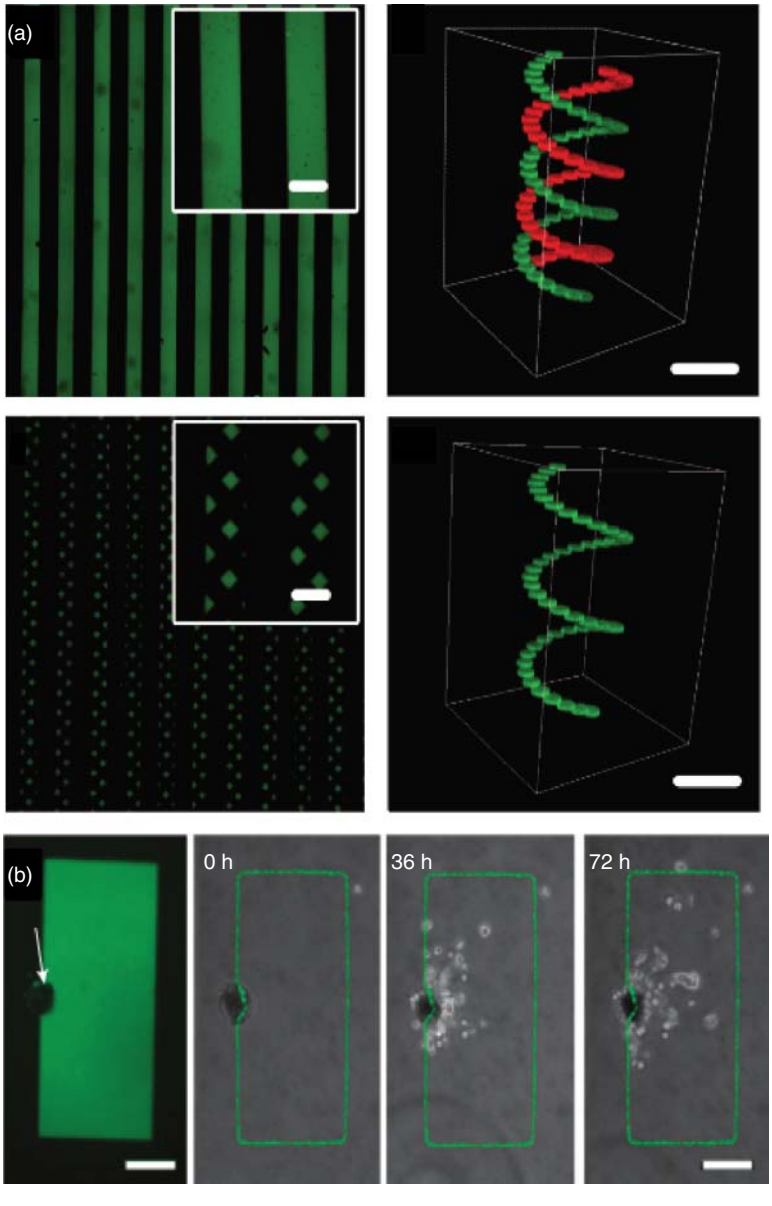

Figure 8.9 Photopatterned modulation of network biochemical properties has been achieved within 3D gels and in the presence of cells using MPL through a variety of chemistries. (a) Sequential thiol–ene coupling and *o*NB photocleavage enables engineered peptides to be reversibly immobilized within a gel network. Scale bars = 200 μm. (DeForest 2011 [184]. Reproduced with permission of Wiley.) (b) Factor XIII-mediated peptide patterning directs mesenchymal stem cell outgrowth into a 3D structure. Scale bars = 200 μm. (Mosiewicz 2013 [104]. Reproduced with permission of Nature Publishing Group.)

such cues. By combining a visible-light-mediated thiol–ene addition reaction with a UV-mediated *o*NB cleavage, DeForest and Anseth demonstrated the reversible biochemical functionalization of a polymer-based material (Figure 8.9b) [184]. This approach allowed dynamic control over cell attachment to a material surface by introducing and, subsequently, removing adhesive ligands from the hydrogel in the presence of cells.

Photochemical reactions have also proven advantageous in controlling network biomechanics in the presence of cells. Strategies to increase culture platform compliance have focused on the photochemical increase in material crosslinking density. The radical chain photopolymerization of (meth)acrylates has been utilized to increase culture stiffness in the presence of cells [26, 190]. Through these same chemistries, photochemical alteration in network enzymatic degradability has enabled spatial control over mesenchymal stem cell differentiation (Figure 8.10a) [193, 194]. Thiol moieties have been photocaged in order to delay additional crosslinking with reactive vinyl groups upon exposure to light. These materials have been shown to influence the migration of human mesenchymal stem cells (hMSCs) [195].

Material stiffness can also be decreased through the use of photochemical reactions. The Anseth group has demonstrated extensively the bulk and local photodegradation of materials in the presence of live cells through the introduction of an *o*NB moiety in the backbone of hydrogel networks (Figure 8.10b) [70, 133, 134]. In a similar approach, coumarin moieties introduced into hydrogel backbones yielded visible-light-degradable materials [143]. The ability to control the mechanical properties of a gel dynamically has been used to guide cell migration and outgrowth [70, 133, 143], to probe cytoskeletal tension within cells (Figure 8.10c) [136], to assess biomechanical memory of hMSCs [137] and in a growing list of other applications.

Photochemical reactions have demonstrated precise control over many critical aspects of the cellular microenvironment, including those both chemical and physical in nature. Through the usage of MPL, micrometer-scale tunability in such parameters has been demonstrated. Given the size scale of a typical mammalian cell (~10 μm), we expect these strategies to prove useful in modulating material properties about individual cells and in better understanding biological response to dynamic extracellular signals.

8.7 Biological Design Constraints

In general, when fabricating materials with MPL photopolymerization, it is critical to balance the power needed to initiate polymerization against the power that will damage or cavitate the precursor solution. For a PEG-based hydrogel, it was found that pulse energies in excess of 2.3 nJ induced cavitation within the highly water swollen gel [136]. When material fabrication or modification is conducted in the presence of cells or organisms, it is also necessary to balance the photophysics of

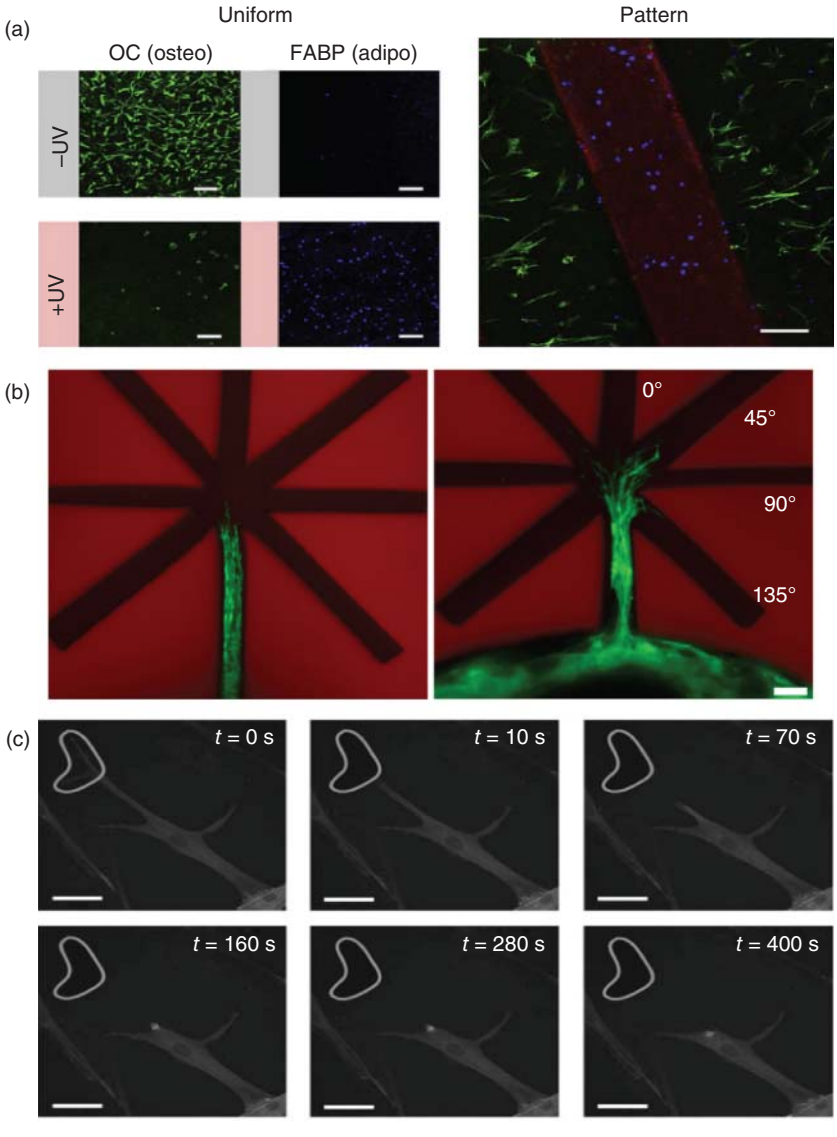

Figure 8.10 Photochemical alteration in network biomechanics has proven an indispensable tool in directing and understanding cell fate. (a) Patterned sequential network crosslinking has afforded spatial control over mesenchymal stem cell differentiation. Scale bars = 100 μm. (Khetan 2010 [191]. Reproduced with permission of Elsevier.) (b,c) MPL has been utilized to photodegrade complex channels within 3D gels [192] and to probe cytoskeletal tension within cells. Scale bars = 100 μm in (b) and 20 μm in (c). (Tibbitt 2010 [136]. Reproduced with permission of Royal Society of Chemistry.)

the reaction with the potential for photodamage to the biological specimen. For instance, it has been shown (and utilized for experimentation) that sufficient pulse energies can sever actin filaments within cells [38, 192, 196]. Additional work has shown that femtosecond pulsed two-photon lasers can be utilized in the presence of cells, but pulse energies above 1.5 nJ induced intracellular photoablation [196] and those above 4 nJ induced cell death [197]. In order to avoid nonspecific damage to intracellular structures and to maintain high cell viability, the experimenter should operate the laser with a pulse energy below 1.5 nJ. As a caveat, these guidelines were determined in non-radical-generating systems and there is the potential for additional cellular damage based on the type and concentration of radicals generated during polymerization. The constraints of biology may further confine the operating space for MPL photopolymerization in the presence of cells; however, the benefit of a small focal volume and little out-of-plane absorption confines potential damage to a narrow window through which the focal point is rastered.

Additional constraints exist in the use of MPL for biological applications. The materials need to be functional and integrate with biological systems, as well as be comprised of components that are compatible with living systems, including each of the constitutive components and potential leachants. While the majority of the chemistries in this chapter have been previously utilized for biomedical applications, novel chemistries should be assessed for compatibility with biological systems.

8.8 Biologic Questions

As advances in MPL fabrication of biocompatible materials are achieved, the class of biomaterials presents unique opportunities to address several questions in biology and regenerative medicine. Both fields are beginning to appreciate the utility of 3D scaffolds for cell culture, as opposed to 2D tissue-culture polystyrene (TCPS), that can better recapitulate critical aspects of the native ECM [198]. Three-dimensional systems facilitate improved tissue morphogenesis and more physiologic culture environments for many cell types of the body [171]. MPL-fabricated materials complement this need for 3D scaffolds, as they can be patterned with micrometer-scale resolution (sub-cellular length scales) that enable researchers to answer questions related to how 3D geometry, topography, and structure affect cell function and tissue organization [199–201]. Several reticulated materials are already being employed for 3D cell culture [172], and, uniquely, MPL allows rapid fabrication of geometrically defined scaffolds as tissue replacements for regenerative medicine. For example, patient-specific devices can be fabricated utilizing medical imaging to assess the geometric need, which can be translated into a digitally rastered structure and printed in a material of interest using MPL.

Excitingly, the ability to manipulate 3D hydrogel biomaterials with MPL (see Section 8.6) uncovers a unique ability to address questions related to how dynamic changes in the ECM influence cell function and tissue assembly. New directions in the field of 4D biology (3D scaffolds that are dynamic in time) rely on user-programmable and externally tunable chemistries to introduce or remove specific cues from the culture microenvironment in real time [15]. Combining these dynamic and user-tunable chemistries with MPL allows the user to control the biophysical and biochemical nature of the cellular environment on the micrometer scale. Similar approaches allow biologists to study how changes in material stiffness influence cell proliferation and differentiation [137] or to investigate how adhesive ligand presentation or removal influences tissue development and function on the cellular level [133]. Additionally, selective photochemistries now allow patterning and removal of bioactive ligands or full proteins to investigate how subcellular localization of specific biochemical moieties may direct intracellular signaling. Moreover, the ability to control these reactions in space and time opens the door to the creation of anisotropic materials and synthetic tissues to study heterogeneous tissue formation and function. Materials scientists and MPL experts must interface and interact with cell and developmental biologists to employ these burgeoning techniques to address critical questions in these fields.

8.9 Outlook

Combining traditional photopolymerization techniques with advances in multiphoton lithography through MPL enables the fabrication of a useful class of photopolymerized biomaterials with defined geometry, architecture, and micrometer-scale features. The broad scope of amenable chemistries for biomaterial and hydrogel synthesis (Section 8.4) and the increasing accessibility of multiphoton technologies will allow MPL-fabricated biomaterials to impact the fields of tissue engineering and regenerative medicine. Specifically, highly defined tissue replacements can be formed from spatially tailored MPL biomaterials for organ therapy. Furthermore, modulatable hydrogels with dynamic subcellular biophysical and biochemical patterning will unlock new understanding in stem cell biology.

As these approaches see continued use and broader applications, there remains a need for an extended toolbox for MPL photopolymerizations. Users will benefit from novel biocompatible photoinitiators with efficient multiphoton cross sections that respond to unique wavelengths. Water-soluble and biocompatible photoinitiators are particularly attractive for hydrogel manipulation via photopatterning in the presence of cells. Additionally, alternative chemistries for the crosslinking of polymer networks and hydrogels that are compatible with cell culture and especially those that facilitate dynamic or reversible crosslinking are desirable. Ideally, contributions will also be made to the toolbox of chemistries that enable multiphoton addition and cleavage reactions within fabricated

biomaterials for advanced studies of how dynamic changes in the biophysical and biochemical nature of the ECM influence cell and tissue function. Expanding this toolbox will require interactions among polymer chemists, photochemists, materials scientists, and biologists to develop advanced techniques for MPL biomaterials.

Continued development on the access to multiphoton sources, which facilitate the necessary techniques for MPL and software that makes these approaches more user-friendly, will also increase use. As the 3D printing industry matures, many of the hardware and software approaches, in principle, can be adopted for advanced photopolymerization approaches via MPL. In total, the outlook for the use of MPL photopolymerizations for the fabrication and modification of biomaterials and hydrogels is bright. Continued interactions at the interface of photopolymerizations, materials science, and biology will allow MPL biomaterials find broad use in the fields of tissue engineering, regenerative medicine, and stem cell biology.

References

1. Lyman, D.J. (1974) Polymers in medicine. *Angew. Chem., Int. Ed. Engl.*, **13**, 108–112.
2. Langer, R. (1998) Drug delivery and targeting. *Nature*, **392**, 5–10.
3. Langer, R. and Vacanti, J.P. (1993) Tissue engineering. *Science*, **260**, 920–926.
4. Langer, R. and Peppas, N.A. (2003) Advances in biomaterials, drug delivery, and bionanotechnology. *AIChE J.*, **49**, 2990–3006.
5. Oster, G. and Yang, N.L. (1968) Photopolymerization of vinyl monomers. *Chem. Rev.*, **68**, 125–151.
6. Anseth, K.S., Bowman, C.N., and Peppas, N.A. (1994) Polymerization kinetics and volume relaxation behavior of photopolymerized multifunctional monomers producing highly crosslinked networks. *J. Polym. Sci. Part A - Polym. Chem.*, **32**, 139–147.
7. Burdick, J.A. and Anseth, K.S. (2002) Photoencapsulation of osteoblasts in injectable rgd-modified peg hydrogels for bone tissue engineering. *Biomaterials*, **23**, 4315–4323.
8. Dorkenoo, K.D., Klein, S., Bombenger, J.P., Barsella, A., Mager, L., and Fort, A. (2006) Functionalized photopolymers for integrated optical components. *Mol. Cryst. Liq. Cryst.*, **446**, 151–160.
9. Fouassier, J.P., Allonas, X., and Burget, D. (2003) Photopolymerization reactions under visible lights: principle, mechanisms and examples of applications. *Prog. Org. Coat.*, **47**, 16–36.
10. Decker, C. (1987) Uv-curing chemistry – past, present, and future. *J. Coat. Technol.*, **59**, 97–106.
11. Nguyen, K.T. and West, J.L. (2002) Photopolymerizable hydrogels for tissue engineering applications. *Biomaterials*, **23**, 4307–4314.
12. Peppas, N.A., Hilt, J.Z., Khademhosseini, A., and Langer, R. (2006) Hydrogels in biology and medicine: from molecular principles to bionanotechnology. *Adv. Mater.*, **18**, 1345–1360.
13. Juodkazis, S., Mizeikis, V., and Misawa, H. (2009) Three-dimensional microfabrication of materials by femtosecond lasers for photonics applications. *J. Appl. Phys.*, **106**, 051101.
14. Bates, C.M., Maher, M.J., Janes, D.W., Ellison, C.J., and Willson, C.G. (2014) Block copolymer lithography. *Macromolecules*, **47**, 2–12.
15. Tibbitt, M.W. and Anseth, K.S. (2012) Dynamic microenvironments: the fourth dimension. *Sci. Transl. Med.*, **4**, 160ps24.

16. Lovestead, T.M., O'Brien, A.K., and Bowman, C.N. (2003) Models of multivinyl free radical photopolymerization kinetics. *J. Photochem. Photobiol. A: Chem.*, **159**, 135–143.
17. Goodner, M.D. and Bowman, C.N. (2002) Development of a comprehensive free radical photopolymerization model incorporating heat and mass transfer effects in thick films. *Chem. Eng. Sci.*, **57**, 887–900.
18. Elisseeff, J., Anseth, K., Sims, D., McIntosh, W., Randolph, M., and Langer, R. (1999) Transdermal photopolymerization for minimally invasive implantation. *Proc. Natl. Acad. Sci. U.S.A.*, **96**, 3104–3107.
19. Sebra, R.P., Masters, K.S., Bowman, C.N., and Anseth, K.S. (2005) Surface grafted antibodies: controlled architecture permits enhanced antigen detection. *Langmuir*, **21**, 10907–10911.
20. Bratton, D., Yang, D., Dai, J.Y., and Ober, C.K. (2006) Recent progress in high resolution lithography. *Polym. Adv. Technol.*, **17**, 94–103.
21. Zhang, X., Jiang, X.N., and Sun, C. (1999) Micro-stereolithography of polymeric and ceramic microstructures. *Sens. Actuators, A: Phys.*, **77**, 149–156.
22. Xia, Y.N. and Whitesides, G.M. (1998) Soft lithography. *Annu. Rev. Mater. Sci.*, **28**, 153–184.
23. Guan, J.J., Ferrell, N., Lee, L.J., and Hansford, D.J. (2006) Fabrication of polymeric microparticles for drug delivery by soft lithography. *Biomaterials*, **27**, 4034–4041.
24. Khademhosseini, A., Langer, R., Borenstein, J., and Vacanti, J.P. (2006) Microscale technologies for tissue engineering and biology. *Proc. Natl. Acad. Sci. U.S.A.*, **103**, 2480–2487.
25. Kane, R.S., Takayama, S., Ostuni, E., Ingber, D.E., and Whitesides, G.M. (1999) Patterning proteins and cells using soft lithography. *Biomaterials*, **20**, 2363–2376.
26. Hahn, M.S., Miller, J.S., and West, J.L. (2006) Three-dimensional biochemical and biomechanical patterning of hydrogels for guiding cell behavior. *Adv. Mater.*, **18**, 2679–2684.
27. Marder, S.R., Bredas, J.-L., and Perry, J.W. (2007) Materials for multiphoton 3d microfabrication. *MRS Bull.*, **32**, 561–565.
28. Malinauskas, M., Farsari, M., Piskarskas, A., and Juodkazis, S. (2013) Ultrafast laser nanostructuring of photopolymers: a decade of advances. *Phys. Rep.: Rev. Sect. Phys. Lett.*, **533**, 1–31.
29. Pawlicki, M., Collins, H.A., Denning, R.G., and Anderson, H.L. (2009) Two-photon absorption and the design of two-photon dyes. *Angew. Chem. Int. Ed.*, **48**, 3244–3266.
30. Zipfel, W.R., Williams, R.M., and Webb, W.W. (2003) Nonlinear magic: multiphoton microscopy in the biosciences. *Nat. Biotechnol.*, **21**, 1369–1377.
31. Kawata, S., Sun, H.B., Tanaka, T., and Takada, K. (2001) Finer features for functional microdevices - micromachines can be created with higher resolution using two-photon absorption. *Nature*, **412**, 697–698.
32. Li, Z., Torgersen, J., Ajami, A., Muehleder, S., Qin, X., Husinsky, W., Holnthoner, W., Ovsianikov, A., Stampfl, J., and Liska, R. (2013) Initiation efficiency and cytotoxicity of novel water-soluble two-photon photoinitiators for direct 3d microfabrication of hydrogels. *RSC Adv.*, **3**, 15939–15946.
33. Klein, F., Richter, B., Striebel, T., Franz, C.M., von Freymann, G., Wegener, M., and Bastmeyer, M. (2011) Two-component polymer scaffolds for controlled three-dimensional cell culture. *Adv. Mater.*, **23**, 1341–1345.
34. Denk, W., Strickler, J.H., and Webb, W.W. (1990) Two-photon laser scanning fluorescence microscopy. *Science*, **248**, 73–76.
35. Xu, C., Zipfel, W., Shear, J.B., Williams, R.M., and Webb, W.W. (1996) Multiphoton fluorescence excitation: new spectral windows for biological nonlinear microscopy. *Proc. Natl. Acad. Sci. U.S.A.*, **93**, 10763–10768.
36. Denk, W. (1994) Two-photon scanning photochemical microscopy - mapping ligand gated ion-channel distributions. *Proc. Natl. Acad. Sci. U.S.A.*, **91**, 6629–6633.

37. Majewska, A., Tashiro, A., and Yuste, R. (2000) Regulation of spine calcium dynamics by rapid spine motility. *J. Neurosci.*, **20**, 8262–8268.
38. Kumar, S., Maxwell, I.Z., Heisterkamp, A., Polte, T.R., Lele, T.P., Salanga, M., Mazur, E., and Ingber, D.E. (2006) Viscoelastic retraction of single living stress fibers and its impact on cell shape, cytoskeletal organization, and extracellular matrix mechanics. *Biophys. J.*, **90**, 3762–3773.
39. Farsari, M., Vamvakaki, M., and Chichkov, B.N. (2010) Multiphoton polymerization of hybrid materials. *J. Opt.*, **12**, 124001.
40. Sun, H.B., Xu, Y., Juodkazis, S., Sun, K., Watanabe, M., Matsuo, S., Misawa, H., and Nishii, J. (2001) Arbitrary-lattice photonic crystals created by multiphoton microfabrication. *Opt. Lett.*, **26**, 325–327.
41. He, G.S., Tan, L.-S., Zheng, Q., and Prasad, P.N. (2008) Multiphoton absorbing materials: molecular designs, characterizations, and applications. *Chem. Rev.*, **108**, 1245–1330.
42. Culver, J.C., Hoffmann, J.C., Poche, R.A., Slater, J.H., West, J.L., and Dickinson, M.E. (2012) Three-dimensional biomimetic patterning in hydrogels to guide cellular organization. *Adv. Mater.*, **24**, 2344–2348.
43. Odian, G.G. (2004) *Principles of Polymerization*, 4th edn, John Wiley & Sons, Inc., Hoboken, NJ, p. xxiv, 812 pp.
44. Aujard, I., Benbrahim, C., Gouget, M., Ruel, O., Baudin, J.-B., Neveu, P., and Jullien, L. (2006) O-Nitrobenzyl photolabile protecting groups with red-shifted absorption: syntheses and uncaging cross-sections for one- and two-photon excitation. *Chem.-A Eur. J.*, **12**, 6865–6879.
45. Kiskin, N.I., Chillingworth, R., McCray, J.A., Piston, D., and Ogden, D. (2002) The efficiency of two-photon photolysis of a "caged" fluorophore, o-1-(2-nitrophenyl)ethylpyranine, in relation to photodamage of synaptic terminals. *Eur. Biophys. J. Biophys. Lett.*, **30**, 588–604.
46. Scranton, A.B., Bowman, C.N., Klier, J., and Peppas, N.A. (1992) Polymerization reaction dynamics of ethylene-glycol methacrylates and dimethacrylates by calorimetry. *Polymer*, **33**, 1683–1689.
47. Goodner, M.D. and Bowman, C.N. (1999) Modeling primary radical termination and its effects on autoacceleration in photopolymerization kinetics. *Macromolecules*, **32**, 6552–6559.
48. Andrzejewska, E. (2001) Photopolymerization kinetics of multifunctional monomers. *Prog. Polym. Sci.*, **26**, 605–665.
49. Kloxin, A.M., Kloxin, C.J., Bowman, C.N., and Anseth, K.S. (2010) Mechanical properties of cellularly responsive hydrogels and their experimental determination. *Adv. Mater.*, **22**, 3484–3494.
50. Fouassier, J.-P. and Lalevée, J. (2012) *Photoinitiators for Polymer Synthesis: Scope, Reactivity and Efficiency*, Wiley-VCH Verlag GmbH, Weinheim, p. xxviii, 476 pp.
51. Bryant, S.J., Nuttelman, C.R., and Anseth, K.S. (2000) Cytocompatibility of Uv and visible light photoinitiating systems on cultured Nih/3t3 fibroblasts in vitro. *J. Biomater. Sci. Polym. Ed.*, **11**, 439–457.
52. Cadet, J., Berger, M., Douki, T., Morin, B., Raoul, S., Ravanat, J.L., and Spinelli, S. (1997) Effects of Uv and visible radiation on DNA – final base damage. *Biol. Chem.*, **378**, 1275–1286.
53. Nakagawa, A., Kobayashi, N., Muramatsu, T., Yamashina, Y., Shirai, T., Hashimoto, M.W., Ikenaga, M., and Mori, T. (1998) Three-dimensional visualization of ultraviolet-induced DNA damage and its repair in human cell nuclei. *J. Invest. Dermatol.*, **110**, 143–148.
54. Fouassier, J.P., Burr, D., and Wieder, F. (1991) Water-soluble photoinitiators – primary processes in hydroxy alkyl phenyl ketones. *J. Polym. Sci. Part A-Polym. Chem.*, **29**, 1319–1327.
55. Majima, T., Schnabel, W., and Weber, W. (1991) Phenyl-2,4,6-trimethylbenzoylphosphinates as water-soluble photoinitiators – generation and

reactivity of O=P(C6h5)(O-) radical-anions. *Makromol. Chem.-Macromol. Chem. Phys.*, **192**, 2307–2315.

56. Fairbanks, B.D., Schwartz, M.P., Bowman, C.N., and Anseth, K.S. (2009) Photoinitiated polymerization of PEG-diacrylate with lithium phenyl-2,4,6-trimethylbenzoylphosphinate: polymerization rate and cytocompatibility. *Biomaterials*, **30**, 6702–6707.

57. Ifkovits, J.L. and Burdick, J.A. (2007) Review: photopolymerizable and degradable biomaterials for tissue engineering applications. *Tissue Eng.*, **13**, 2369–2385.

58. Jakubiak, J. and Rabek, J.F. (1999) Photoinitiators for visible light polymerization. *Polimery*, **44**, 447–461.

59. Shi, W.F. and Ranby, B. (1996) Photopolymerization of dendritic methacrylated polyesters.1. Synthesis and properties. *J. Appl. Polym. Sci.*, **59**, 1937–1944.

60. Dworak, C., Koch, T., Varga, F., and Liska, R. (2010) Photopolymerization of biocompatible phosphorus-containing vinyl esters and vinyl carbamates. *J. Polym. Sci. Part A: Polym. Chem.*, **48**, 2916–2924.

61. Heller, C., Schwentenwein, M., Russmueller, G., Koch, T., Moser, D., Schopper, C., Varga, F., Stampfl, J., and Liska, R. (2011) Vinylcarbonates and vinylcarbamates: biocompatible monomers for radical photopolymerization. *J. Polym. Sci. Part A: Polym. Chem.*, **49**, 650–661.

62. Hoyle, C.E. and Bowman, C.N. (2010) Thiol-ene click chemistry. *Angew. Chem. Int. Ed.*, **49**, 1540–1573.

63. Heller, C., Schwentenwein, M., Russmueller, G., Varga, F., Stampfl, J., and Liska, R. (2009) Vinyl esters: low cytotoxicity monomers for the fabrication of biocompatible 3D scaffolds by lithography based additive manufacturing. *J. Polym. Sci. Part A-Polym. Chem.*, **47**, 6941–6954.

64. Slaughter, B.V., Khurshid, S.S., Fisher, O.Z., Khademhosseini, A., and Peppas, N.A. (2009) Hydrogels in regenerative medicine. *Adv. Mater.*, **21**, 3307–3329.

65. Hoffman, A.S. (2002) Hydrogels for biomedical applications. *Adv. Drug Delivery Rev.*, **54**, 3–12.

66. Lee, K.Y. and Mooney, D.J. (2001) Hydrogels for tissue engineering. *Chem. Rev.*, **101**, 1869–1879.

67. von Sonntag, C. (1991) The chemistry of free-radical-mediated DNA damage. *Basic Life Sci.*, **58**, 287–317; discussion -21.

68. Sawhney, A.S., Pathak, C.P., and Hubbell, J.A. (1993) Bioerodible hydrogels based on photopolymerized poly(ethylene glycol)-co-poly(alpha-hydroxy acid) diacrylate macromers. *Macromolecules*, **26**, 581–587.

69. Hoyle, C.E., Lee, T.Y., and Roper, T. (2004) Thiol-enes: chemistry of the past with promise for the future. *J. Polym. Sci. Part A-Polym. Chem.*, **42**, 5301–5338.

70. DeForest, C.A. and Anseth, K.S. (2011) Cytocompatible click-based hydrogels with dynamically tunable properties through orthogonal photocoupling and photodegradation reactions. *Nat. Chem.*, **3**, 925–931.

71. Fairbanks, B.D., Schwartz, M.P., Halevi, A.E., Nuttelman, C.R., Bowman, C.N., and Anseth, K.S. (2009) A versatile synthetic extracellular matrix mimic via thiol-norbornene photopolymerization. *Adv. Mater.*, **21**, 5005–5010.

72. Aimetti, A.A., Machen, A.J., and Anseth, K.S. (2009) Poly(ethylene glycol) hydrogels formed by thiol-ene photopolymerization for enzyme-responsive protein delivery. *Biomaterials*, **30**, 6048–6054.

73. Munoz, Z., Shih, H., and Lin, C.C. (2014) Gelatin hydrogels formed by orthogonal thiol-norbornene photochemistry for cell encapsulation. *Biomater. Sci.*, **2**, 1063–1072.

74. Mergy, J., Fournier, A., Hachet, E., and Auzely-Velty, R. (2012) Modification of polysaccharides via thiol-ene chemistry: a versatile route to functional biomaterials. *J. Polym. Sci. Part A-Polym. Chem.*, **50**, 4019–4028.

75. Aimetti, A.A., Feaver, K.R., and Anseth, K.S. (2010) Synthesis of cyclic, multivalent arg-gly-asp using sequential

thiol-ene/thiol-yne photoreactions. *Chem. Commun.*, **46**, 5781–5783.
76. DeForest, C.A., Polizzotti, B.D., and Anseth, K.S. (2009) Sequential click reactions for synthesizing and patterning three-dimensional cell microenvironments. *Nat. Mater.*, **8**, 659–664.
77. DeForest, C.A., Sims, E.A., and Anseth, K.S. (2010) Peptide-functionalized click hydrogels with independently tunable mechanics and chemical functionality for 3D cell culture. *Chem. Mater.*, **22**, 4783–4790.
78. Malkoch, M., Vestberg, R., Gupta, N., Mespouille, L., Dubois, P., Mason, A.F., Hedrick, J.L., Liao, Q., Frank, C.W., Kingsbury, K., and Hawker, C.J. (2006) Synthesis of Well-defined hydrogel networks using click chemistry. *Chem. Commun.*, 2774–2776.
79. Hoogenboom, R. (2010) Thiol-yne chemistry: a powerful tool for creating highly functional materials. *Angew. Chem. Int. Ed.*, **49**, 3415–3417.
80. Chen, G.J., Kumar, J., Gregory, A., and Stenzel, M.H. (2009) Efficient synthesis of dendrimers via a thiol-yne and esterification process and their potential application in the delivery of platinum anti-cancer drugs. *Chem. Commun.*, 6291–6293.
81. Konkolewicz, D., Gray-Weale, A., and Perrier, S. (2009) Hyperbranched polymers by thiol-yne chemistry: from small molecules to functional polymers. *J. Am. Chem. Soc.*, **131**, 18075–18077.
82. Fairbanks, B.D., Scott, T.F., Kloxin, C.J., Anseth, K.S., and Bowman, C.N. (2009) Thiol-yne photopolymerizations: novel mechanism, kinetics, and step-growth formation of highly crosslinked networks. *Macromolecules*, **42**, 211–217.
83. Fairbanks, B.D., Sims, E.A., Anseth, K.S., and Bowman, C.N. (2010) Reaction rates and mechanisms for radical, photoinitated addition of thiols to alkynes, and implications for thiol-yne photopolymerizations and click reactions. *Macromolecules*, **43**, 4113–4119.
84. Meldal, M. (2008) Polymer "clicking" by cuAAC reactions. *Macromol. Rapid Commun.*, **29**, 1016–1051.
85. Rostovtsev, V.V., Green, L.G., Fokin, V.V., and Sharpless, K.B. (2002) A stepwise huisgen cycloaddition process: copper(I)-catalyzed regioselective "Ligation" of azides and terminal alkynes. *Angew. Chem. Int. Ed.*, **41**, 2596–2599.
86. Tornoe, C.W., Christensen, C., and Meldal, M. (2002) Peptidotriazoles on solid phase: [1,2,3]-triazoles by regiospecific copper(I)-catalyzed 1,3-dipolar cycloadditions of terminal alkynes to azides. *J. Org. Chem.*, **67**, 3057–3064.
87. Adzima, B.J., Tao, Y., Kloxin, C.J., DeForest, C.A., Anseth, K.S., and Bowman, C.N. (2011) Spatial and temporal control of the alkyne-azide cycloaddition by photoinitiated Cu(II) reduction. *Nat. Chem.*, **3**, 258–261.
88. Gong, T., Adzima, B.J., Baker, N.H., and Bowman, C.N. (2013) Photopolymerization reactions using the photoinitiated copper (I)-catalyzed azide-alkyne cycloaddition (CuAAC) reaction. *Adv. Mater.*, **25**, 2024–2028.
89. Baskin, J.M., Prescher, J.A., Laughlin, S.T., Agard, N.J., Chang, P.V., Miller, I.A., Lo, A., Codelli, J.A., and Bertozzi, C.R. (2007) Copper-free click chemistry for dynamic in vivo imaging. *Proc. Natl. Acad. Sci. U.S.A.*, **104**, 16793–16797.
90. Agard, N.J., Prescher, J.A., and Bertozzi, C.R. (2004) A strain-promoted [3 + 2] azide-alkyne cycloaddition for covalent modification of biomolecules in living systems. *J. Am. Chem. Soc.*, **126**, 15046–15047.
91. Poloukhtine, A.A., Mbua, N.E., Wolfert, M.A., Boons, G.J., and Popik, V.V. (2009) Selective labeling of living cells by a photo-triggered click reaction. *J. Am. Chem. Soc.*, **131**, 15769–15776.
92. Arumugam, S., Orski, S.V., Mbua, N.E., McNitt, C., Boons, G.J., Locklin, J., and Popik, V.V. (2013) Photo-click chemistry strategies for spatiotemporal control of metal-free ligation, labeling, and surface derivatization. *Pure Appl. Chem.*, **85**, 1499–1513.
93. Orski, S.V., Poloukhtine, A.A., Arumugam, S., Mao, L.D., Popik, V.V., and Locklin, J. (2010) High density orthogonal surface immobilization

via photoactivated copper-free click chemistry. *J. Am. Chem. Soc.*, **132**, 11024–11026.

94. McNitt, C.D. and Popik, V.V. (2012) Photochemical generation of oxa-dibenzocyclooctyne (ODIBO) for metal-free click ligations. *Org. Biomol. Chem.*, **10**, 8200–8202.
95. Pauloehrl, T., Delaittre, G., Bruns, M., Meissler, M., Borner, H.G., Bastmeyer, M., and Barner-Kowollik, C. (2012) (Bio)molecular surface patterning by phototriggered oxime ligation. *Angew. Chem. Int. Ed.*, **51**, 9181–9184.
96. Dendane, N., Hoang, A., Guillard, L., Defrancq, E., Vinet, F., and Dumy, P. (2007) Efficient surface patterning of oligonucleotides inside a glass capillary through oxime bond formation. *Bioconjugate Chem.*, **18**, 671–676.
97. Park, S. and Yousaf, M.N. (2008) An interfacial oxime reaction to immobilize ligands and cells in patterns and gradients to photoactive surfaces. *Langmuir*, **24**, 6201–6207.
98. Mancini, R.J., Li, R.C., Tolstyka, Z.P., and Maynard, H.D. (2009) Synthesis of a photo-caged aminooxy alkane thiol. *Org. Biomol. Chem.*, **7**, 4954–4959.
99. Luo, Y. and Shoichet, M.S. (2004) A photolabile hydrogel for guided three-dimensional cell growth and migration. *Nat. Mater.*, **3**, 249–253.
100. Wosnick, J.H. and Shoichet, M.S. (2008) Three-dimensional chemical patterning of transparent hydrogels. *Chem. Mater.*, **20**, 55–60.
101. Wylie, R.G., Ahsan, S., Aizawa, Y., Maxwell, K.L., Morshead, C.M., and Shoichet, M.S. (2011) Spatially controlled simultaneous patterning of multiple growth factors in three-dimensional hydrogels. *Nat. Mater.*, **10**, 799–806.
102. Xi, W.X., Krieger, M., Kloxin, C.J., and Bowman, C.N. (2013) A new photoclick reaction strategy: photo-induced catalysis of the thiol-michael addition via a caged primary amine. *Chem. Commun.*, **49**, 4504–4506.
103. Liu, Z.Z., Lin, Q.N., Sun, Y., Liu, T., Bao, C.Y., Li, F.Y., and Zhu, L.Y. (2014) Spatiotemporally controllable and cytocompatible approach builds 3D cell culture matrix by photo-uncaged-thiol michael addition reaction. *Adv. Mater.*, **26**, 3912–3917.
104. Mosiewicz, K.A., Kolb, L., Vlies, A.J.V.D., Martino, M.M., Lienemann, P.S., Hubbell, J.A., Ehrbar, M., and Lutolf, M.P. (2013) In situ cell manipulation through enzymatic hydrogel photopatterning. *Nat. Mater.*, **12**, 1072–1078.
105. Griffin, D.R., Borrajo, J., Soon, A., Acosta-Velez, G.F., Oshita, V., Darling, N., Mack, J., Barker, T., Iruela-Arispe, M.L., and Segura, T. (2014) Hybrid photopatterned enzymatic reaction (hyper) for in situ cell manipulation. *ChemBioChem*, **15**, 233–242.
106. Gilchrist, T.L. and Rees, C.W. (1969) *Carbenes Nitrenes and Arynes (Studies in Modern Chemistry)*, Appleton-Century-Crofts.
107. Kotzybahibert, F., Kapfer, I., and Goeldner, M. (1995) Recent trends in photoaffinity-labeling. *Angew. Chem., Int. Ed. Engl.*, **34**, 1296–1312.
108. Chin, J.W., Santoro, S.W., Martin, A.B., King, D.S., Wang, L., and Schultz, P.G. (2002) Addition of p-azido-L-phenylaianine to the genetic code of Escherichia coli. *J. Am. Chem. Soc.*, **124**, 9026–9027.
109. Carrico, I.S., Maskarinec, S.A., Heilshorn, S.C., Mock, M.L., Liu, J.C., Nowatzki, P.J., Franck, C., Ravichandran, G., and Tirrell, D.A. (2007) Lithographic patterning of photoreactive cell-adhesive proteins. *J. Am. Chem. Soc.*, **129**, 4874–4875.
110. Smith, J.W. and Cheresh, D.A. (1988) The Arg-Gly-Asp binding domain of the vitronectin receptor – photoaffinity cross-linking implicates amino-acid residues-61-203 of the beta-subunit. *J. Biol. Chem.*, **263**, 18726–18731.
111. Smith, R.A.G. and Knowles, J.R. (1973) Aryldiazirines – potential reagents for photolabeling of biological receptor sites. *J. Am. Chem. Soc.*, **95**, 5072–5073.
112. Hoppe, J., Brunner, J., and Jorgensen, B.B. (1984) Structure of the membrane-embedded F0 part of F1f0 ATP synthase from Escherichia-coli as inferred

from labeling with 3-(trifluoromethyl)-3-(m-[I-125]iodophenyl)diazirine. *Biochemistry*, **23**, 5610–5616.

113. Harter, C., James, P., Bachi, T., Semenza, G., and Brunner, J. (1989) Hydrophobic binding of the ectodomain of influenza hemagglutinin to membranes occurs through the fusion peptide. *J. Biol. Chem.*, **264**, 6459–6464.

114. Raphel, J., Parisi-Amon, A., and Heilshorn, S.C. (2012) Photoreactive elastin-like proteins for use as versatile bioactive materials and surface coatings. *J. Mater. Chem.*, **22**, 19429–19437.

115. Brunner, J. and Semenza, G. (1981) Selective labeling of the hydrophobic core of membranes with 3-(trifluoromethyl)-3-(m-[I-125]iodophenyl)diazirine, a carbene-generating reagent. *Biochemistry*, **20**, 7174–7182.

116. Vanderbend, R.L., Brunner, J., Jalink, K., Vancorven, E.J., Moolenaar, W.H., and Vanblitterswijk, W.J. (1992) Identification of a putative membrane-receptor for the bioactive phospholipid, lysophosphatidic acid. *EMBO J.*, **11**, 2495–2501.

117. Walling, C. and Gibian, M. (1965) Hydrogen abstraction reactions by the triplet states of ketones. *J. Am. Chem. Soc.*, **87**, 3361.

118. Dorman, G. and Prestwich, G.D. (1994) Benzophenone photophores in biochemistry. *Biochemistry*, **33**, 5661–5673.

119. Prucker, O., Naumann, C.A., Ruhe, J., Knoll, W., and Frank, C.W. (1999) Photochemical attachment of polymer films to solid surfaces via monolayers of benzophenone derivatives. *J. Am. Chem. Soc.*, **121**, 8766–8770.

120. Herbert, C.B., McLernon, T.L., Hypolite, C.L., Adams, D.N., Pikus, L., Huang, C.C., Fields, G.B., Letourneau, P.C., Distefano, M.D., and Hu, W.S. (1997) Micropatterning gradients and controlling surface densities of photoactivatable biomolecules on self-assembled monolayers of oligo(ethylene glycol) alkanethiolates. *Chem. Biol.*, **4**, 731–737.

121. Balakirev, M.Y., Porte, S., Vernaz-Gris, M., Berger, M., Arie, J.P., Fouque, B., and Chatelain, F. (2005) Photochemical patterning of biological molecules inside a glass capillary. *Anal. Chem.*, **77**, 5474–5479.

122. Rich, D.H. and Gurwara, S.K. (1973) Removal of protected peptides from an ortho-nitrobenzyl resin by photolysis. *J. Chem. Soc. Chem. Commun.*, 610–611.

123. Zhao, Y., Zheng, Q., Dakin, K., Xu, K., Martinez, M.L., and Li, W.H. (2004) New caged coumarin fluorophores with extraordinary uncaging cross sections suitable for biological imaging applications. *J. Am. Chem. Soc.*, **126**, 4653–4663.

124. Holmes, C.P. and Jones, D.G. (1995) Reagents for combinatorial organic-synthesis – development of a new O-nitrobenzyl photolabile linker for solid-phase synthesis. *J. Org. Chem.*, **60**, 2318–2319.

125. Holmes, C.P. (1997) Model studies for new O-nitrobenzyl photolabile linkers: substituent effects on the rates of photochemical cleavage. *J. Org. Chem.*, **62**, 2370–2380.

126. Griffin, D.R., Schlosser, J.L., Lam, S.F., Nguyen, T.H., Maynard, H.D., and Kasko, A.M. (2013) Synthesis of photodegradable macromers for conjugation and release of bioactive molecules. *Biomacromolecules*, **14**, 1199–1207.

127. Wu, Y.I., Frey, D., Lungu, O.I., Jaehrig, A., Schlichting, I., Kuhlman, B., and Hahn, K.M. (2009) A genetically encoded photoactivatable rac controls the motility of living cells. *Nature*, **461**, 104-U11.

128. Deiters, A. (2010) Principles and applications of the photochemical control of cellular processes. *ChemBioChem*, **11**, 47–53.

129. Ohmuro-Matsuyama, Y. and Tatsu, Y. (2008) Photocontrolled cell adhesion on a surface functionalized with a caged arginine-glycine-aspartate peptide. *Angew. Chem. Int. Ed.*, **47**, 7527–7529.

130. Kaneko, S., Nakayama, H., Yoshino, Y., Fushimi, D., Yamaguchi, K., Horiike, Y., and Nakanishi, J. (2011) Photocontrol of cell adhesion on amino-bearing

surfaces by reversible conjugation of poly(ethylene glycol) via a photocleavable linker. *Phys. Chem. Chem. Phys.*, **13**, 4051–4059.

131. Johnson, J.A., Finn, M.G., Koberstein, J.T., and Turro, N.J. (2007) Synthesis of photocleavable linear macromonomers by atrp and star macromonomers by a tandem atrp-click reaction: precursors to photodegradable model networks. *Macromolecules*, **40**, 3589–3598.
132. Johnson, J.A., Baskin, J.M., Bertozzi, C.R., Koberstein, J.T., and Turro, N.J. (2008) Copper-free click chemistry for the in situ crosslinking of photodegradable star polymers. *Chem. Commun.*, 3064–3066.
133. Kloxin, A.M., Kasko, A.M., Salinas, C.N., and Anseth, K.S. (2009) Photodegradable hydrogels for dynamic tuning of physical and chemical properties. *Science*, **324**, 59–63.
134. Kloxin, A.M., Tibbitt, M.W., and Anseth, K.S. (2010) Synthesis of photodegradable hydrogels as dynamically tunable cell culture platforms. *Nat. Protoc.*, **5**, 1867–1887.
135. Kloxin, A.M., Benton, J.A., and Anseth, K.S. (2010) In situ elasticity modulation with dynamic substrates to direct cell phenotype. *Biomaterials*, **31**, 1–8.
136. Tibbitt, M.W., Kloxin, A.M., Dyamenahalli, K.U., and Anseth, K.S. (2010) Controlled Two-photon photodegradation of PEG hydrogels to study and manipulate subcellular interactions on soft materials. *Soft Matter*, **6**, 5100–5108.
137. Yang, C., Tibbitt, M.W., Basta, L., and Anseth, K.S. (2014) Mechanical memory and dosing influence stem cell fate. *Nat. Mater.*, **13**, 645–652.
138. Schade, B., Hagen, V., Schmidt, R., Herbrich, R., Krause, E., Eckardt, T., and Bendig, J. (1999) Deactivation behavior and excited-state properties of (coumarin-4-yl)methyl derivatives. 1. Photocleavage of (7-methoxycoumarin-4-yl)methyl-caged acids with fluorescence enhancement. *J. Org. Chem.*, **64**, 9109–9117.
139. Geissler, D., Antonenko, Y.N., Schmidt, R., Keller, S., Krylova, O.O., Wiesner, B., Bendig, J., Pohl, P., and Hagen, V. (2005) (Coumarin-4-yl)methyl esters as highly efficient, ultrafast phototriggers for protons and their application to acidifying membrane surfaces. *Angew. Chem. Int. Ed.*, **44**, 1195–1198.
140. Schmidt, R., Geissler, D., Hagen, V., and Bendig, J. (2007) Mechanism of photocleavage of (coumarin-4-yl)methyl esters. *J. Phys. Chem. A*, **111**, 5768–5774.
141. Mal, N.K., Fujiwara, M., and Tanaka, Y. (2003) Photocontrolled reversible release of guest molecules from coumarin-modified mesoporous silica. *Nature*, **421**, 350–353.
142. Babin, J., Pelletier, M., Lepage, M., Allard, J.F., Morris, D., and Zhao, Y. (2009) A new two-photon-sensitive block copolymer nanocarrier. *Angew. Chem. Int. Ed.*, **48**, 3329–3332.
143. Azagarsamy, M.A., McKinnon, D.D., Age, D.L., and Anseth, K.S. (2014) Coumarin-based photodegradable hydrogel: design, synthesis, gelation, and degradation kinetics. *ACS Macro Lett.*, **3**, 515–519.
144. Azagarsamy, M.A. and Anseth, K.S. (2013) Wavelength-controlled photocleavage for the orthogonal and sequential release of multiple proteins. *Angew. Chem. Int. Ed.*, **52**, 13803–13807.
145. Bonifacic, M. and Asmus, K.D. (1984) Adduct formation and absolute rate constants in the displacement reaction of thiyl radicals with disulfides. *J. Phys. Chem.*, **88**, 6286–6290.
146. Tobolsky, A.V., Takahashi, M., and Macknight, W.J. (1964) Relaxation of disulfide and tetrasulfide polymers. *J. Phys. Chem.*, **68**, 787–790.
147. Fairbanks, B.D., Singh, S.P., Bowman, C.N., and Anseth, K.S. (2011) Photodegradable, photoadaptable hydrogels via radical-mediated disulfide fragmentation reaction. *Macromolecules*, **44**, 2444–2450.
148. Bowen, E.J. and Tanner, D.W. (1955) The photochemistry of anthracenes. 3. Inter-relations between fluorescence quenching, dimerization, and photo-oxidation. *Trans. Faraday Soc.*, **51**, 475–481.

149. Odonnell, M. (1968) Photodimerization of solid anthracene. *Nature*, **218**, 460–461.
150. Chandros, E.A. (1965) Photolytic dissociation of dianthracene. *J. Chem. Phys.*, **43**, 4175–4176.
151. Wells, L.A., Brook, M.A., and Sheardown, H. (2011) Generic, anthracene-based hydrogel crosslinkers for photo-controllable drug delivery. *Macromol. Biosci.*, **11**, 988–998.
152. Sako, Y. and Takaguchi, Y. (2008) A photo-responsive hydrogelator having gluconamides at its peripheral branches. *Org. Biomol. Chem.*, **6**, 3843–3847.
153. Zheng, Y.J., Mieie, M., Mello, S.V., Mabrouki, M., Andreopoulos, F.M., Konka, V., Pham, S.M., and Leblanc, R.M. (2002) Peg-based hydrogel synthesis via the photodimerization of anthracene groups. *Macromolecules*, **35**, 5228–5234.
154. Frank, P.G., Tuten, B.T., Prasher, A., Chao, D.M., and Berda, E.B. (2014) Intra- chain photodimerization of pendant anthracene units as an effi cient route to single- chain nanoparticle fabrication. *Macromol. Rapid Commun.*, **35**, 249–253.
155. Chiefari, J., Chong, Y.K., Ercole, F., Krstina, J., Jeffery, J., Le, T.P.T., Mayadunne, R.T.A., Meijs, G.F., Moad, C.L., Moad, G., Rizzardo, E., and Thang, S.H. (1998) Living free-radical polymerization by reversible addition-fragmentation chain transfer: the raft process. *Macromolecules*, **31**, 5559–5562.
156. Meijs, G.F., Rizzardo, E., and Thang, S.H. (1988) Preparation of controlled molecular-weight, olefin-terminated polymers by free-radical methods – chain transfer using allylic sulfides. *Macromolecules*, **21**, 3122–3124.
157. Meijs, G.F., Morton, T.C., Rizzardo, E., and Thang, S.H. (1991) Use of substituted allylic sulfides to prepare end-functional polymers of controlled molecular-weight by free-radical polymerization. *Macromolecules*, **24**, 3689–3695.
158. Moad, G., Rizzardo, E., and Thang, S.H. (2008) Radical addition-fragmentation chemistry in polymer synthesis. *Polymer*, **49**, 1079–1131.
159. Scott, T.F., Schneider, A.D., Cook, W.D., and Bowman, C.N. (2005) Photoinduced plasticity in cross-linked polymers. *Science*, **308**, 1615–1617.
160. Kloxin, C.J., Scott, T.F., Adzima, B.J., and Bowman, C.N. (2010) Covalent adaptable networks (cans): a unique paradigm in cross-linked polymers. *Macromolecules*, **43**, 2643–2653.
161. Gandavarapu, N.R., Azagarsamy, M.A., and Anseth, K.S. (2014) Photo-click living strategy for controlled, reversible exchange of biochemical ligands. *Adv. Mater.*, **26**, 2521–2526.
162. Li, L. and Fourkas, J.T. (2007) Multiphoton polymerization. *Mater. Today*, **10**, 30–37.
163. Coenjarts, C.A. and Ober, C.K. (2004) Two-photon three-dimensional microfabrication of poly(dimethylsiloxane) elastomers. *Chem. Mater.*, **16**, 5556–5558.
164. Adzima, B.J., Kloxin, C.J., DeForest, C.A., Anseth, K.S., and Bowman, C.N. (2012) 3D photofixation lithography in Diels-Alder networks. *Macromol. Rapid Commun.*, **33**, 2092–2096.
165. Serbin, J., Egbert, A., Ostendorf, A., Chichkov, B.N., Houbertz, R., Domann, G., Schulz, J., Cronauer, C., Frohlich, L., and Popall, M. (2003) Femtosecond laser-induced two-photon polymerization of inorganic-organic hybrid materials for applications in photonics. *Opt. Lett.*, **28**, 301–303.
166. Lee, W.M., Pruzinsky, S.A., and Braun, P.V. (2002) Multi-photon polymerization of waveguide structures within three-dimensional photonic crystals. *Adv. Mater.*, **14**, 271–274.
167. Klein, S., Barsella, A., Leblond, H., Bulou, H., Fort, A., Andraud, C., Lemercier, G., Mulatier, J.C., and Dorkenoo, K. (2005) One-step waveguide and optical circuit writing in photopolymerizable materials processed by two-photon absorption. *Appl. Phys. Lett.*, **86**, 211118-1.
168. Guo, R., Xiao, S.Z., Zhai, X.M., Li, J.W., Xia, A.D., and Huang, W.H. (2006) Micro lens fabrication by means of

femtosecond two photon photopolymerization. *Opt. Express*, **14**, 810–816.
169. Yokoyama, S., Nakahama, T., Miki, H., and Mashiko, S. (2003) Fabrication of three-dimensional microstructure in optical-gain medium using two-photon-induced photopolymerization technique. *Thin Solid Films*, **438**, 452–456.
170. Daley, W.P., Peters, S.B., and Larsen, M. (2008) Extracellular matrix dynamics in development and regenerative medicine. *J. Cell Sci.*, **121**, 255–264.
171. Tibbitt, M.W. and Anseth, K.S. (2009) Hydrogels as extracellular matrix mimics for 3D cell culture. *Biotechnol. Bioeng.*, **103**, 655–663.
172. Torgersen, J., Qin, X.-H., Li, Z., Ovsianikov, A., Liska, R., and Stampfl, J. (2013) Hydrogels for two-photon polymerization: a toolbox for mimicking the extracellular matrix. *Adv. Funct. Mater.*, **23**, 4542–4554.
173. Doraiswamy, A., Jin, C., Narayan, R.J., Mageswaran, P., Mente, P., Modi, R., Auyeung, R., Chrisey, D.B., Ovsianikov, A., and Chichkov, B. (2006) Two photon induced polymerization of organic-inorganic hybrid biomaterials for microstructured medical devices. *Acta Biomater.*, **2**, 267–275.
174. Claeyssens, F., Hasan, E.A., Gaidukeviciute, A., Achilleos, D.S., Ranella, A., Reinhardt, C., Ovsianikov, A., Xiao, S., Fotakis, C., Vamvakaki, M., Chichkov, B.N., and Farsari, M. (2009) Three-dimensional biodegradable structures fabricated by two-photon polymerization. *Langmuir*, **25**, 3219–3223.
175. Qin, X.-H., Torgersen, J., Saf, R., Muehleder, S., Pucher, N., Ligon, S.C., Holnthoner, W., Redl, H., Ovsianikov, A., Stampfl, J., and Liska, R. (2013) Three-dimensional microfabrication of protein hydrogels via two-photon-excited thiol-vinyl ester photopolymerization. *J. Polym. Sci. Part A-Polym. Chem.*, **51**, 4799–4810.
176. Kaehr, B. and Shear, J.B. (2008) Multiphoton fabrication of chemically responsive protein hydrogels for microactuation. *Proc. Natl. Acad. Sci. U.S.A.*, **105**, 8850–8854.
177. Ovsianikov, A., Chichkov, B., Adunka, O., Pillsbury, H., Doraiswamy, A., and Narayan, R.J. (2007) Rapid prototyping of ossicular replacement prostheses. *Appl. Surf. Sci.*, **253**, 6603–6607.
178. Torgersen, J., Ovsianikov, A., Mironov, V., Pucher, N., Qin, X., Li, Z., Cicha, K., Machacek, T., Liska, R., Jantsch, V., and Stampfl, J. (2012) Photo-sensitive hydrogels for three-dimensional laser microfabrication in the presence of whole organisms. *J. Biomed. Opt.*, **17**, 105008.
179. Jhaveri, S.J., McMullen, J.D., Sijbesma, R., Tan, L.-S., Zipfel, W., and Ober, C.K. (2009) Direct three-dimensional microfabrication of hydrogels via two-photon lithography in aqueous solution. *Chem. Mater.*, **21**, 2003–2006.
180. Pitts, J.D., Campagnola, P.J., Epling, G.A., and Goodman, S.L. (2000) Submicron multiphoton free-form fabrication of proteins and polymers: studies of reaction efficiencies and applications in sustained release. *Macromolecules*, **33**, 1514–1523.
181. Pitts, J.D., Howell, A.R., Taboada, R., Banerjee, I., Wang, J., Goodman, S.L., and Campagnola, P.J. (2002) New photoactivators for multiphoton excited three-dimensional submicron cross-linking of proteins: bovine serum albumin and type 1 collagen. *Photochem. Photobiol.*, **76**, 135–144.
182. Kaehr, B., Allen, R., Javier, D.J., Currie, J., and Shear, J.B. (2004) Guiding neuronal development with in situ microfabrication. *Proc. Natl. Acad. Sci. U.S.A.*, **101**, 16104–16108.
183. Leslie-Barbick, J.E., Shen, C., Chen, C., and West, J.L. (2011) Micron-scale spatially patterned, covalently immobilized vascular endothelial growth factor on hydrogels accelerates endothelial tubulogenesis and increases cellular angiogenic responses. *Tissue Eng. Part A*, **17**, 221–229.
184. DeForest, C.A. and Anseth, K.S. (2011) Photoreversible patterning of biomolecules within click-based hydrogels. *Angew. Chem. Int. Ed.*, **51**, 1816–1819.

185. McCall, J.D., Luoma, J.E., and Anseth, K.S. (2012) Covalently tethered transforming growth factor beta in peg hydrogels promotes chondrogenic differentiation of encapsulated human mesenchymal stem cells. *Drug Delivery Transl. Res.*, **2**, 305–312.

186. Salinas, C.N. and Anseth, K.S. (2008) The enhancement of chondrogenic differentiation of human mesenchymal stem cells by enzymatically regulated rgd functionalities. *Biomaterials*, **29**, 2370–2377.

187. Rolli, C.G., Nakayama, H., Yamaguchi, K., Spatz, J.P., Kemkemer, R., and Nakanishi, J. (2012) Switchable adhesive substrates: revealing geometry dependence in collective cell behavior. *Biomaterials*, **33**, 2409–2418.

188. Lin, H.M., Wang, W.K., Hsiung, P.A., and Shyu, S.G. (2010) Light-sensitive intelligent drug delivery systems of coumarin-modified mesoporous bioactive glass. *Acta Biomater.*, **6**, 3256–3263.

189. Hossion, A.M.L., Bio, M., Nkepang, G., Awuah, S.G., and You, Y. (2013) Visible light controlled release of anticancer drug through double activation of prodrug. *ACS Med. Chem. Lett.*, **4**, 124–127.

190. Khetan, S., Katz, J.S., and Burdick, J.A. (2009) Sequential crosslinking to control cellular spreading in 3-dimensional hydrogels. *Soft Matter*, **5**, 1601–1606.

191. Khetan, S. and Burdick, J.A. (2010) Patterning network structure to spatially control cellular remodeling and stem cell fate within 3-dimensional hydrogels. *Biomaterials*, **31**, 8228–8234.

192. McKinnon, D.D., Brown, T.E., Kyburz, K.A., Kiyotake, E., and Anseth, K.S. (2014) Design and characterization of a synthetically accessible photodegradable hydrogel for user-directed formation of neural networks. *Biomacromolecules*, **15**, 2808–2816.

193. Guvendiren, M. and Burdick, J.A. (2012) Stiffening hydrogels to probe short- and long-term cellular responses to dynamic mechanics. *Nat. Commun.*, **3**, 792.

194. Khetan, S., Guvendiren, M., Legant, W.R., Cohen, D.M., Chen, C.S., and Burdick, J.A. (2013) Degradation-mediated cellular traction directs stem cell fate in covalently crosslinked three-dimensional hydrogels. *Nat. Mater.*, **12**, 458–465.

195. Mosiewicz, K.A., Kolb, L., van der Vlies, A.J., and Lutolf, M.P. (2014) Microscale patterning of hydrogel stiffness through light-triggered uncaging of thiols. *Biomater. Sci.*, **2**, 1640–1651.

196. Heisterkamp, A., Maxwell, I.Z., Mazur, E., Underwood, J.M., Nickerson, J.A., Kumar, S., and Ingber, D.E. (2005) Pulse energy dependence of subcellular dissection by femtosecond laser pulses. *Opt. Express*, **13**, 3690–3696.

197. Shen, N., Datta, D., Schaffer, C.B., LeDuc, P., Ingber, D.E., and Mazur, E. (2005) Ablation of cytoskeletal filaments and mitochondria in live cells using a femtosecond laser nanoscissor. *Mech. Chem. Biosyst.*, **2**, 17–25.

198. Watanabe, W., Arakawa, N., Matsunaga, S., Higashi, T., Fukui, K., Isobe, K., and Itoh, K. (2004) Femtosecond laser disruption of subcellular organelles in a living cell. *Opt. Express*, **12**, 4203–4213.

199. Abbott, A. (2003) Cell culture: biology's new dimension. *Nature*, **424**, 870–872.

200. Dalby, M.J., Gadegaard, N., Tare, R., Andar, A., Riehle, M.O., Herzyk, P., Wilkinson, C.D.W., and Oreffo, R.O.C. (2007) The control of human mesenchymal cell differentiation using nanoscale symmetry and disorder. *Nat. Mater.*, **6**, 997–1003.

201. Xiong, F., Ma, W., Hiscock, T.W., Mosaliganti, K.R., Tentner, A.R., Brakke, K.A., Rannou, N., Gelas, A., Souhait, L., Swinburne, I.A., Obholzer, N.D., and Megason, S.G. (2014) Interplay of cell shape and division orientation promotes robust morphogenesis of developing epithelia. *Cell*, **159**, 415–427.